Using statistical analysis to create a new database of Nanofluids' specific heat capacity

Adela Svobodova-Sedlackova[1,2], Alejandro Calderón[1,3], Xavier Sanuy Morell[4], Marc Neira-Viñas[1], Marc Majó[1], Camila Barreneche[1], Pablo Gamallo[1,2] and A. Inés Fernandez[1*]

[1]Departament de Ciència de Materials i Química Física, Universitat de Barcelona, C/Martí i Franqués 1, 08028, Barcelona, Spain.

[2]Institut de Química Teòrica i Computacional, IQTCUB, Universitat de Barcelona, C/Martí i Franqués 1, 08028, Barcelona, Spain.

[3] Departament d'Enginyeria Mecànica, Universitat Rovira i Virgili, Av. Paisos Catalans 26, 43007 Tarragona, Spain

[4]Department of Materials Science and Engineering, the University of Sheffield, Sir Robert Hadfield Building, Mappin St, S1 3JD, Sheffield, UK

*Corresponding author: ana_inesfernandez@ub.edu

Abstract

Nowadays, heat transfer fluids (HTFs) with high thermal properties are needed to develop more efficient and compact energy systems to achieve sustainable development goals. Nanofluids (NFs), through the incorporation of nanoparticles in conventional HTFs, become one of the most suitable techniques to improve their thermophysical properties. However, despite its potential industrial applications, there is not only a lack of a theoretical framework but also a clear trend about its behavior. Therefore, this work aims to perform a critical review and statistical analysis to understand the NFs heat capacity (*Cp*). To this end, a wide variety of NFs from the literature was processed using Principal Component Analysis (PCA) and Response Surface Methodology (RSM). Finally, a database with Ansys Granta Constructor 2021 software was created and an analysis with Ansys Granta Selector 2021 was performed. As a result, the key parameters that impact the *Cp* of several nanofluids are obtained as well as: their high-temperature dependence, the nature of the liquid medium, and the type of nanoparticles. In addition, the results allow to identify and design nanofluids with specific properties for specific working conditions.

Keywords: Nanofluids; Concentrated Solar Power (CSP); Thermal Energy Storage (TES); nanoparticles; Principal Component Analysis (PCA); Response Surface Methodology (RSM).

1. Introduction

Energy is an essential resource for humanity, and its storage is one of the fundamental points for industrial development. Energy storage is considered a key factor for ~~enabling technology for~~ fully implementing renewable energies (RE)~~, solving their main drawback,~~ and facilitating sustainable development goals. Therefore, incorporating a storage system allows to implement more efficient, safe, and flexible systems [1,2]. In ~~P~~particular, concentrated solar power (CSP) plants that incorporate thermal energy storage (TES) facilities have become one of the most promising renewable solar technologies due to their cost-efficiency relation [3,4]. Several parameters of working fluids must be considered to design more efficient systems. Usually, these working fluids are simultaneously used as TES materials and/or as heat transfer fluids (HTF). Therefore, the design, development, and improvement of TES and HTF fluids are essential for developing high-efficiency and optimal systems [5].

In the last years, researchers in diverse fields have been interested in the improvement of thermophysical properties observed in fluids when ~~across the addition of~~ nanoparticles (NPs) were added into ~~fluids~~ (*i.e.,* oils [6], polyethylene glycol [7], molten salts [8], water [9]). This fact encourage researchers to develop a new class of fluids known as nanofluids (NFs), studied for the first time in 1995 by Choi S. *et al.* [10]. NFs are engineered by suspending nanoparticles (NPs) ~~(~~ that are between 1 nm and ~~–~~100 nm~~)~~ in diameter in a base fluid. The NP~~s~~ materials can be metallic, non-metallic, oxides, carbides, ceramics, carbon based, a mixture of ~~different NPs~~ them known as ~~(~~hybrid NFs~~)~~, and even nanoscale liquid droplets [11–14]. The NFs show improved thermophysical properties such as heat and mass transfer, thermal conductivity (κ), or specific heat capacity (*Cp*) compared to the base fluid [15–17]. Furthermore, a large variety of new potential applications of NFs have emerged over time, such as: lubricants [18], desalination [19], CO_2 absorption/capture [20], batteries [21], industrial cooling [22], or heat exchangers [23], among others.

Specifically, NFs attracted the scientific community's attention due to their anomalous *Cp* improvement, reaching enhancements up to 30-40 % ~~with~~ by the addition in low concentrations of ~~low~~ NPs ~~concentrations~~ (*i.e.*, 1 wt.%) [24]. Several studies have been carried out in recent years to investigate the NFs *Cp* enhancement, and great advances have been made to understand the phenomena~~on~~ behind [25]. Moreover, the main parameters and properties that influence the *Cp* variation have been identified in the last years: temperature and pH along with ~~NPs parameters (*i.e.,* the~~ concentration, size, shape, or nature of the NPs~~), temperature, and pH mainly, among others~~ [16,26]. Nevertheless, to achieve its scalability and understand its full potential, further investigations are required in order to develop a strong theoretical framework. Despite this, no studies have been found ~~in which a~~ addressed to clarify the trend observed in *Cp* values ~~is showed~~ [16]. In addition, there is a high dispersion on the experimental-measured data

reported in the literature.~~:~~ Thus, there are experiments that under the same experimental conditions ~~show~~ report different *Cp* values and performance. Furthermore, the results are contradictory in many cases, with unclear trends ~~on their behavior~~ [27–32]. Therefore, there are not clear tendencies on how the incorporation of NPs affects *Cp*. Another difficulty seen in the literature is the few specifications and non-accurate descriptions of the measurements and calculation methods. For example, there is no information that indicate at which temperature thermal values were obtained, or which methodology was followed for preparing the NF. As a result, there does not seem to be a clear specification or protocol for properly measuring NFs. These facts make the comparison of results and the comprehension of their thermal performance under real conditions a challenging task.

This study aims to perform a critical review and analysis to understand the NFs *Cp* experimental reported data. For this purpose, several parameters from NFs employed in energy storage applications were collected from the literature~~:~~ such as base fluid and NPs material, size~~,~~ and concentration of the NPs, temperature, *Cp* enhancement, sampling, and experimental procedure ~~(*i.e.,*~~ related to the equipment and methodology as well~~)~~. Furthermore, a principal component analysis (PCA), ANOVA test, and response surface methodology (RSM) were employed to determine the main parameters affecting the *Cp* and their behavior and to develop a mathematical model. The Ansys Granta Constructor 2021 tool was used to create a database which was analyzed using Ansys Granta Selector 2021 to select NFs with specific properties and to observe their behavior. The main goal of this study is to unify *Cp* values and to identify clear trends to design NFs for applications with specific thermal requirements.

2. Methodology

Data acquisition: The data source for this study ~~groups~~ covers scientific journals and conference proceedings from Scopus database that contain the keywords ~~. The search was effectuated under the following keywords:~~ "Nanofluids" and "Energy Storage~~.~~". ~~There were~~ Up to 2020, a total of 301 publications fulfil these requirements ~~associated with this research topic at the end of 2020,~~ and 111 of them ~~articles included~~ reported *Cp* values. Exactly, a total of 884 *Cp* values and their measurement specifications were extracted from these studies.

Principal component analysis (PCA): the database was standardized by the StandardScaler Sklearn function to make an equal comparison ~~between~~ among all ~~each~~ values [33]. Afterwards, the database was transformed by a principal component analysis (PCA) defined ~~by Sklearn~~ in Ref. [33]. PCA is a statistical method used for dimensionality reduction, features extraction, or data visualization by an orthogonal transformation of the dataset into a new subspace, with new axes called principal components (PCs) [34–36].

Statistical analysis-response surface methodology (RSM): The data were evaluated by the ANOVA statistical analysis ~~(analysis of the variance)~~ to fit the data to a mathematical model ~~and predict values~~. To this end, the dependent variable ~~(response)~~ was the specific heat capacity, and the independent variables, the nanoparticles' size, concentration, and the fluid temperature. In this manner, with the help of Stat-Ease code, an experiment designer software, ~~the design of experiments software (Stat-Ease)~~ ADD REFERENCE! and the obtained equations, a response surface was ¿¿analyzed or obtained??. As a result, the developed models using the experimental responses exhibited p-values below 0.0001, implying that the proposed models are relevant considering the factor relations presented for each response or equation.

Ansys Granta 2021 Constructor/Selector database: The database was created with the Constructor software from Ansys (ADD REFERENCE!), employing the data obtained from the literature. The general organization of the database was divided into inorganic, organic, and mixtures and then arranged depending on the base fluid or the type of nanoparticles. The base fluids considered were hydrocarbons, substituted hydrocarbons, ionic liquids, molten salts, oils, organic acids, water~~,~~ and mixtures~~,~~ whereas ~~And~~ the nanoparticles treated were those formed by metal oxides, metals, nitrides~~,~~ and carbon-based materials ~~nanoparticles~~. **Figure 1** depicts the arrangement of nanofluids~~,~~ and the nanoparticles used ~~in~~ for each base fluid.

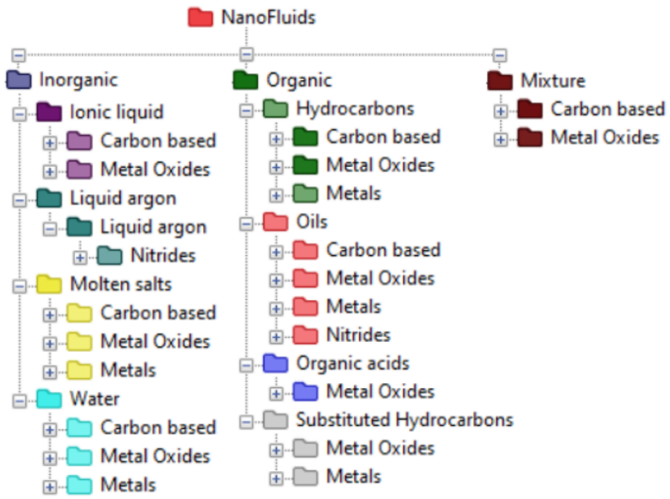

Figure 1. Arrangement of nanofluids in the nanofluids database.

3. Results

NFs were studied for diverse applications as HTS or TES materials~~.~~ although each application needs different thermal requirements. According to this fact, these applications ~~can be~~ have been classified as high, medium, or low temperature [37]. ~~Therefore, each application needs different thermal requirements.~~ For this reason, a great variety of base fluid materials were

found in the literature quest ~~research~~. More in detail, **Table 1** summarizes the obtained 36 base fluids, with their corresponding references. It is important noting ~~Point out~~ that solar salt (*i.e.*, $NaNO_3$ – KNO_3 (60:40)) and water were the most studied systems ~~and from which~~ , so reporting the highest amount of ~~more~~ *Cp* values ~~were obtained~~.

Table 1. Summary of nanofluid~~s~~ base materials collected from ~~the~~ literature ~~and their corresponding references.~~

Base material	References
Distilled Water (DW)	[45][46]
Methoxyperfluorobutane (HFE 7100)	[70]
Water	[70][71][72][73][74][75][76][77] [78][79][80][81][47][82][48][83] [84] [85]
Propylene glycol (PG)	[53]
Capric acid (CA)	[86]
Myristic acid-capric acid eutectic (MA-CA)	[86]
Paraffin	[87][88][89]
n-octadecane	[49]
Polyalphaolefein (PAO)	[90][91]
Engine oil	[92][93][46][94]
Heat transfer oil	[95]
Mineral oil	[90]
Therminol-55	[96]
Oleic acid-(DL-menthol)	[97]
ethylene glycol (EG)	[51][50][98][94][46][84][90][99]
Glycerol	[99]
EG/Water	[100][101][102][103][72][90] [104][105][106][45][107][108]
KNO_3	[109][110][111]
$NaNO_3$	[4] [25] [59]
$NaNO_3$– KNO_3 (60:40)	[112][113][114][28][115][30][11 6][117][29][118][119][120][121] [122][123][124][125][126][127] [128][129][130][131] [132][133][27][134][135][60] [61] [110][136][62]
$BaCl_2$– H_2O	[137]
NaCl-$CaCl_2$	[138]
$BaCl_2$-NaCl-$CaCl_2$-LiCl	[139]
$Ca(NO_3)\cdot 4H_2O$-$NaNO_3$-KNO_3-$LINO_3$	[30]
$Ca(NO_3)_2$-KNO_3-$NaNO_3$-$LiNO_3$	[140][141][32]
$Na_2CO_3\cdot 10H_2O\cdot Na_2HPO_4\cdot 12H_2O$ EHS (Eutectic Hydrate salt)	[142]
KNO_3–$NaNO_2$– $NaNO_3$ (53:40:7 mol. %) (MHS)	[143]
K_2CO_3-$LiCO_3$-Na_2CO_3	[144]
Li_2CO_3-K_2CO_3	[145][146][147][148][63][64] [65] [66][67][68][69][149]
$LiNO_3$-$NaNO_3$-KNO_3	[30][150][151]
Aviation turbine fuel	[152]
Ionic liquid [C_4mim][PF_6]	[153]
Ionic liquid ~~(~~[Hmim]BF_4~~)~~	[154]
Ionic liquid ~~(~~[C_4mim][NTf_2]	[155]
Ionic liquid [C_4mpyrr][NTf_2]	[155]

For each scientific article, the ~~obtained~~ selected information was the following: base fluid type (BF), ~~density~~ base fluid density (ρ (BF), kg·m³), NPs type, NPs morphology (form factor), NPs concentration (wt. % and/or v. %), NPs density (ρ (NPs), kg·m³), NPs size (S, nm), temperature (T, °C) ~~at was measured the~~ of *Cp* mesurement, *Cp* of BF ($J \cdot K^{-1}$), *Cp* of NF ($J \cdot K^{-1}$), NFs *Cp* variation ($\Delta Cp,\%$)~~,~~ along with the measurement conditions and procedures~~.~~ ~~Measurement conditions and procedures~~ that include the measurement methods, ~~measurement~~ techniques, sampling, and ~~measurement~~ conditions (*i.e.,* whether the first measurement was discarded or not). These variables are critical to analyzing the *Cp* measurement methodology and to allow ~~to compare~~ comparing results ~~values~~ and developing standard methods for characterizing NFs.

3.1. Specific Heat capacity methodology and procedures

Instrumental and methodological analysis*:* Several techniques were found in the literature review to measure the *Cp*. These ~~can be~~ techniques are classified as theoretical (10.18 %) and experimental (89.82 %) ~~techniques. The experimental techniques include a~~ being the latter transient Double Hot-Wire (DHW), thermal conductivity instrument, simultaneous Thermogravimetry Analysis-Differential Scanning Calorimetry (TGA-DSC), Modulated Differential Scanning Calorimetry (MDSC), handmade setups, and Differential Scanning calorimetry (DSC). Otherwise, theoretical techniques include numerical procedures and simulations (*i.e.,* Molecular Dynamics (MD) Ssimulations ~~(MD)~~). **Figure 2** shows ~~a pie chart of the different techniques. The~~ the most used equipment ~~was~~ is DSC, accounting more than 68 % of ~~data measured~~ measurements through this technique. The rest of ~~the~~ techniques represent the 30.1 %: transient DHW (6.4 %), thermal conductivity instrument (0.6 %), simultaneous TGA-DSC (5.4 %), numerical techniques (5.9 %), MDSC (6.9 %), MD simulations (1.2 %) and in-house devices (3.2 %). However, an important remark is that 1.9 % of the data do not describe the technique used to measure the thermophysical properties. Although this is a small proportion, it creates a gap in the methodological procedure since this parameter is essential ~~has to be described in the papers~~ to reproduce the experiments ~~under the same conditions~~. In fact, it is not surprising that the DSC was the most employed technique because it is the most precise and suitable instrument to determine thermal properties (*i.e.,* melting temperature, melting enthalpy, or *Cp*) [38,39]. More in detail, the most used calorimetry instruments (DSC) were manufactured by Mettler Toledo© (26.5 %) and TA Instruments© (22.7 %), representing almost 50 % of the data, followed by Netzsch-Gruppe© (15.2), PerkinElmer®, Inc. (8.6 %) and finally, Setaram KEP technologies, Inc. ® (5.2 %).

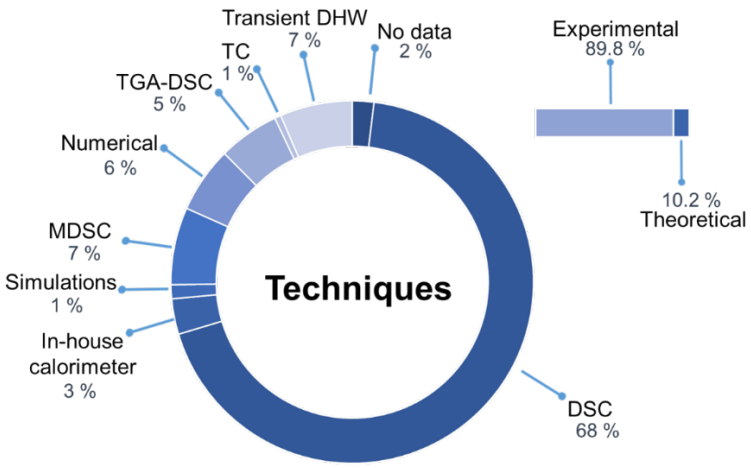

Figure 2. ~~A pie chart of t~~Techniques used to determine the specific heat capacity and the percentage of usage: transient DHW, TC (thermal conductivity instrument), simultaneous TGA-DSC, numerical techniques, MDSC (Modulated Differential scanning calorimeter), MD simulations, in-house calorimeters, DSC~~, and percentage of no data~~. Those determinations that do not specify the technique used are accounted as *no data*. On the right side is the ~~rate of~~ ratio of experimental and theoretical *Cp* determinations.

~~Otherwise, the analysis of the measurement methods followed by each instrumental technique is~~ Another important characteristic ~~to~~ considered is the analysis method followed. Thus, six different methods were identified and categorized into three main groups according to the technique. ~~The pie chart shown in~~ **Figure 3** presents the ratio (%) of data measured following each method: (1) transient DHW: T-history (1.4 %); (2) Thermal conductivity instrument, numerical, MD simulations and in-house setups equations (13.7 %); (3) TGA-DSC, MDSC and DSC techniques: direct method (11.9 %), ASTM E2716 (6.2 %), ASTM E1269 (46.7 %) and the area method (6.1 %). Finally, a total of 124 *Cp* values (14 %) does not indicate the methodology used. In this case, it is remarkable that the lack of information is higher than ~~the ones for the~~ in the case of the instrumental section. This fact generates uncertainty in the data and an incomplete methodological description because the results cannot be further replicated.

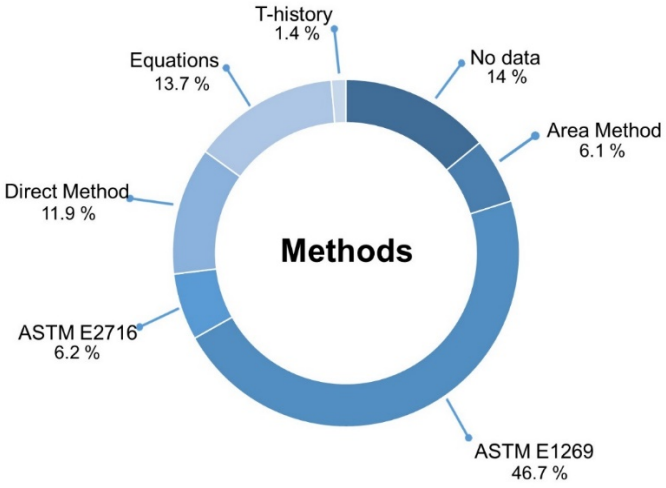

Figure 3. ~~A pie chart of~~ Methods followed to determine the specific heat capacity: ASTM E1269, ~~No data,~~ equations??, direct and area method, ASTM E2716, ~~Area Method,~~ and T-history. Those determinations that do not specify the technique used are accounted as *no data*.

~~This fact generates uncertainty in the data and an incomplete methodological description because the results cannot be replicated.~~

Despite this, the most applied methodology is a standard procedure, "*Standard Test Method for Determining Specific Heat Capacity by Differential Scanning Calorimetry*" [40] by ASTM International. Therefore, following standardized procedures helps to compare results with ~~each~~ other studies. Otherwise, the second main group corresponds to the *Cp* determination through equations QUÉ SIGNIFICA!!! (13.7 %), followed by the direct method in DSC (11.9 %). Moreover, the area method (6.1 %) and the standard methodology ASTM E2716 "Standard Test Method for Determining Specific Heat Capacity by Sinusoidal Modulated Temperature Differential Scanning Calorimetry" [41] (6.2 %) shows a similar ratio. Lastly, the less-used method is the T-history (1.4%) which has been used in the transient DHW technique. In addition, **Table 2** summarizes the relevant equations used to determine *Cp* for all the described methods.

Table 2. Equation~~'s~~ description of the specific heat capacity methods~~: Model I, Model II, in-house calorimeter, diffusivity, effective volumetric specific heat, effective specific heat, simulations, Debye theory, ASTM E1269, ASTM E2716.~~

Method	Formula
Model I	$C_{p,nf} = \emptyset \cdot C_{p,s} + (1 - \emptyset) \cdot C_{p,bf} \quad (eq.1)$ $C_{p,nf}$= specific heat capacity of the nanofluid. $C_{p,s}$= solid particle specific heat capacity. $\emptyset$ = particle volumetric concentration and $C_{p,bf}$= base fluid specific heat.
Model II	$C_{p,nf} = \frac{\emptyset \cdot \rho_s \cdot C_{p,s} + (1 - \emptyset) \cdot \emptyset \cdot \rho_{bf} \cdot C_{p,bf}}{\rho_{nf}} \quad (eq.2)$ ρ_s=solid particles density. ρ_{bf} =base fluid density and ρ_{nf} =nanofluid density.

Effective volumetric specific heat	$$(\rho C_p)_{nf} = [\, \emptyset_p \cdot \rho_p \cdot C_{p-p} + (1-\emptyset_p) \cdot \rho_f \cdot C_{p-f}] \qquad (eq.3)$$ $\emptyset$= particle volumetric concentration and subscript *nf* indicate the nanofluid, *p* the nanoparticle, and *f* the base fluid.
Effective specific heat	$$C_{p\,-nf} = \frac{[\, \emptyset_p \cdot \rho_p \cdot C_{p-p} + (1-\emptyset_p) \cdot \rho_f \cdot C_{p-f}]}{\emptyset_p \cdot \rho_p + (1-\emptyset_p) \cdot \rho_f} \qquad (eq.4)$$ $\emptyset$= particle volumetric concentration and subscript *nf* indicate the nanofluid, *p* the nanoparticle, and *f* the base fluid.
In-house calorimeter	$$C_{p,nf} = \frac{\dot{Q} \cdot \Delta t - m_c \cdot C_{pc} \cdot \Delta T_c - m_{co} \cdot C_{p,co} \cdot \Delta T_{co} - m_{IN} \cdot C_{p,IN} \cdot \Delta T_{IN} - \dot{q}_L \cdot \Delta t}{m_{nf} \cdot \Delta T_{nf}} \; (eq.5)$$ $\dot{Q}$= heat applied, Δt = interval time (s), ΔT= temperature rise (K), m= mass (kg), *Cp*= specific heat capacity, $\dot{q}_L$= heat transfer to the environment~~.~~ ~~and the~~ Subscript~~s~~ *C* indicates the container, *CO* the heating coil, and *IN* the insulator~~ion~~.
Diffusivity	$$C_{p-nf} = \frac{k_{nf}}{\alpha_{nf} \cdot \rho_{nf}} \qquad (eq.6)$$ $$\rho_{nf} = \emptyset \cdot \rho_p + (1-\emptyset_p) \cdot \rho_f \qquad (eq.7)$$ k_{nf}= thermal conductivity, α_{nf}= thermal diffusivity, ρ_{nf} = nanofluid density, $\emptyset$= particle volumetric concentration, ρ_p= particles density and ρ_f= fluid density.
MD simulations	$$C_p = (\frac{\partial E}{\partial T})_p = \frac{\langle \delta E^2 \rangle_{NPT}}{k_B \cdot T^2} \qquad (eq.8)$$ k_B= Boltzmann constant, *T*= temperature, E= total internal energy and C_p= specific heat capacity.
Debye theory (Phonon heat capacity)	$$C_v = \frac{1}{\rho V K_B T^2} \sum_{\vec{q},p} \frac{(\hbar\omega_{\vec{q},p})^2 e^{\frac{\hbar\omega_{\vec{q},p}}{K_B T}}}{(e^{\frac{\hbar\omega_{\vec{q},p}}{K_B T}} - 1)^2} \qquad (eq.9)$$ C_v= specific heat capacity at constant volume, k_B= Boltzmann constant, *T*= temperature, $\hbar\omega_{\vec{q},p}$ = phonon energy, ρ =density and V =volume.
ASTM E1269	$$C_p = C_{p,sapphire} \cdot \frac{\Delta q_s \cdot m_{sapphire}}{\Delta q_{sapphire} \cdot m_s} = C_{p,sapphire} \cdot \frac{(q_s - q_o) \cdot m_{sapphire}}{(q_{sapphire} - q_o) \cdot m_s} \qquad (eq.10)$$ C_p= specific heat capacity, q = heat flow, m= mass, and subscript *s* indicates samples (pure mixtures or nanomaterials) and *st* the standard materials.
ASTM E2716	$$C_{p,rev} = \frac{A_{mhf}}{W_s \cdot A_{mrh}} \qquad (eq.11)$$ $$T = T_o + \beta \cdot T + A_{mhr} \cdot \sin(wt) \qquad (eq.12)$$ $$C_{p,non} = \frac{\langle P \rangle}{W_s \cdot \beta} - C_{p,rev} \qquad (eq.13)$$ $C_{p,rev}$ = reversing component of the apparent specific heat, A_{mhf}= amplitude of the first harmonic of the heat flow, A_{mrh} =amplitude of the applied heating rate, W_s = mass sample, β= heating rate, A_{mhr} = amplitude of the perturbation, w =frequency of the perturbation, *T*= sample temperature, t =time, $\langle P \rangle$ =average heat flow, and $C_{p,non}$ =non-reversing specific heat.
Areas Method	$$C_{p,m} = \frac{C_{p,s} \cdot A_m}{A_s} \qquad (eq.14)$$ $$A_s = \frac{\dot{Q}_S}{m_S} = C_{p,s} \cdot \beta \qquad (eq.15)$$ $$A_s = \frac{\dot{Q}_m}{m_m} = C_{p,m} \cdot \beta \qquad (eq.16)$$ A_s = Integrated peak area for the sapphire curve, A_m= integrated peak area for the material curve, $C_{p,s}$ =sapphire specific heat capacity, m_S= sapphire sample mass, m_m= material sample mass, $\dot{Q}_S$= the sapphire heat flux signal, $\dot{Q}_m$= material heat flux signal, and β = heating rate.

Direct method	$\dot{Q} = C_p(T) \cdot \beta \quad (eq.17)$ $\dot{Q}$= Heat flux. $C_p(T)$= specific heat capacity in function of the temperature. β= heating rate.
T-history	$T'_S = \frac{dT_S}{dt} = \frac{h_{air} \cdot A_{surface} \cdot (T_{air} - T_S)}{m_S \cdot C_{p,s}} \quad (eq.18)$ T_{air} =temperature of furnace air, T_S=sample temperature, m_S=sample mass, $C_{p,s}$= specific heat capacity sample

The first eight equations ~~of~~ in Table 2 have been included in the equation methods group-first, the equations formulated for the NFs; Model I, **eq. 1**, was developed by Pak and Cho *et al.* [42] and is based on the liquid-particles mixture theory and the dependency of the particle concentration. However, this model is approximately valid for dilute suspensions when small density differences exist between base fluid and nanoparticles. Xuan and Roetzel *et al.,* [43] modified this correlation by assuming thermal equilibrium between the nanoscale solid particles and the liquid phase, including the density (Model II), **eq.2**. Nevertheless, the literature showed a large gap between the expected values and the values experimentally obtained. Therefore, the values obtained through these models tend to ~~present~~ exhibit a high standard deviation. Derived from these two models, **eq. 3** and **eq. 4** and from the definition of the nanofluids density [44] were defined the effective volumetric specific heat and the effective specific heat of NFs, respectively. On the other hand, **eq. 3** describes the equation mainly used in the in-house calorimeters, as a function of the temperature, time, mass, and the applied heat flux [45]. Another way to determine ~~de~~ the *Cp* was related to its determination through thermal conductivity and thermal diffusivity values, **eqs. 4-5**~~**., eq. 5**~~ [42,46,47].

Alternatively, thermophysical properties can be determined theoretically from MD simulations ~~(*i.e.,* Molecular dynamics simulations, MD). These numerical techniques~~ that use internal energy terms to predict the *Cp*, such as the **eq. 8** [48,49]. Finally, the *Cp* at constant volume can be determined through theoretical models as **eq. 9** describes (Debye theory) [50]. In the same way, **eq.10-17** describe all the methods derived from a calorimetric instrument (*i.e.*, Differential scanning calorimetry technique): direct method, ASTM E2716, ASTM E1269, MDSC, and the areas method. The ASTM E1269 is a standard three-step procedure: the baseline heat flux (q_o) was obtained with two empty-pans as the first step analysis. In the second step, the heat flux of a reference sample with a known *Cp* (*i.e.,* sapphire sample) was measured ($q_{ref/sapphire}$). Finally, in the third step, the sample heat was determined (q_{sample}), and by eq. 10, the *Cp* is obtained [39]. On the other hand, can be used other two methods to determine *Cp* with DSC. First, the area method that consists of two consecutive isothermal segments without a heating stage and a temperature difference of 1 ºC between the isotherms. The signal peak due to the isotherm's temperature differences, see eq. 15, is compared with the area of the known

reference material, eq. 16 (*i.e.,* sapphire), to obtain the *Cp* ~~by the~~ through eq. 14 [39]. Otherwise, the conventional method involves the evaluation of the enthalpy curve, measured within a certain temperature range, being the *Cp* the area under the enthalpy curve ~~represents the *Cp*~~. This is based on the relation between the heat flow rate, the *Cp* at a constant pressure of the sample inside the sample cell, and the scanning rate β, eq. 17 [39]. Finally, the MDSC technique, a variation of the DSC, ~~(which is a DSC variation technique)~~ applies a sinusoidal heat signal (eq. 12), separating the *Cp* into reversing, eq. 11, and non-reversing component, eq.13. The reversing component of the heat flow is obtained from the amplitude of the first harmonic of the heat flow A_{mhf}, through a Fourier transform of the data. Then, the reversing component of the apparent *Cp*, is obtained by dividing the heat flow A_{mhf} by the amplitude of the applied heat rate, A_{mrh}~~,~~ [51,52]. This technique is useful to separate the kinetic contribution (time-dependent factors). Lastly, ~~a~~ the T-history technique determines the *Cp* according to the eq. 18 [53,54]. This method was first developed by Yinping *et al.*, in 1999 [55] and enables to obtain properties like melting point, fusion heat, degree of sub-cooling, thermal conductivity, and specific heat of several samples simultaneously.

Sampling: The high inconsistency about the *Cp* values in the reviewed and reported literature suggest that one of the possible issues that caused the high discrepancy in results was the difficult task of obtaining a good representative sample due to the low concentration of nanoparticles~~' concentration~~. Typically, due to the small amount of sample weight that uses standard calorimetric techniques. For this reason, an analysis of the sampling and statistics followed by researchers was performed. Two main aspects were considered, the number of samples and the number of measurements repetitions per each sample. **Figure 4** summarizes the general trends of the sampling performed in the analyzed literature.

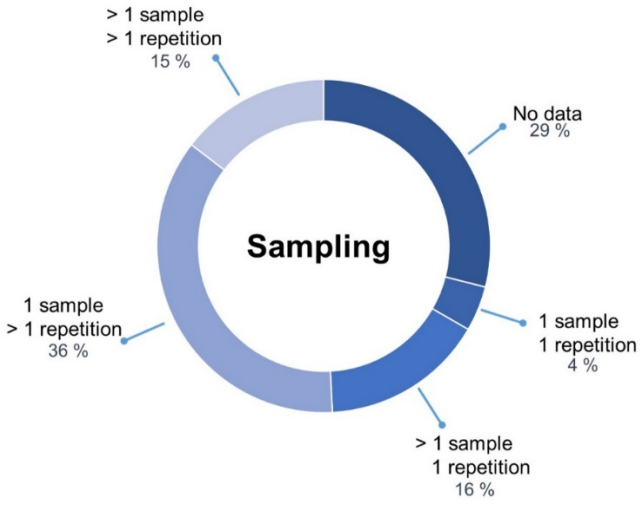

Figure 4. ~~A pie chart of the~~ Sampling done in the revised literature to determine specific nanofluids heat capacity values.

Many *Cp* values were obtained from the analysis of just one sample and by means of more than one measurement repetition (36 %). The choice of this procedure minimizes the effect of non-stability and agglomeration of nanoparticles inside the liquid medium. However, it is not ~~a proper~~ an appropriate ~~measurement~~ procedure from the point of view of sampling and instrumental error because the samples are not ~~there is not a~~ representative ~~sample~~.

~~The opposite~~ Another situation consists in analyzing ~~is the cases where~~ more than one sample ~~was analyzed~~ but only performing one repetition for each sample ~~was run~~. This experimental procedure was ~~used~~ followed for ~~to~~ obtaining 15.8 % of the total data evaluated.

In addition, the most appropriate procedure is the case where more than one sample and more than one repetition is performed and represents 14.6 % of the analyzed cases. This last sampling procedure ~~sh~~would minimize the errors associated to the measurement, the nanoparticle concentration, and the stability of the sample~~, and measurement errors~~. Hence, this procedure is expected to offer high-quality values regarding measurement uncertainty.

Finally, the ~~least desirable~~ the most unfavorable procedure from a statistical point of view ~~is obtained when~~ corresponds to the analysis of only one sample ~~and~~ with just one measurement repetition ~~are~~ performed. This ~~undesirable condition~~ procedure represents ~~only~~ a 4.4 % of the analyzed data.

Nevertheless, sampling procedure of NFs needs to be carried out in order to reduce measurement errors. Thereby, the first step is to develop a methodology to obtain a good representative sample (*i.e.,* quartering) and determine the minimum number of independent samples to minimize ~~a~~ the measurement error due to the inhomogeneity of NFs samples.

As a final fact, a relevant finding is that ~~the~~ 29 % of the data presented in the literature does not report how the *Cp* result was obtained. The lack of that information about experimental procedure is the base to highlight even more that there is significant uncertainty in the reported *Cp* values.

Likewise, it is well known that the particle size of the samples influences the thermophysical properties (*i.e.,* melting temperature, specific heat capacity, …). For this reason, it is crucial first to melt the sample to remove the granulometry effects. In addition, it ensures a better contact of the sample with the bottom of the crucible and removes the air within the sample. As a result, values obtained with a single measurement have low-quality from a statistical point of view. To minimize this effect, it is necessary to perform several measurement repetitions and discard the first analysis (first run) to obtain a more reliable value. From the analyzed data ~~literature~~, only 21 % ~~of the data~~ considered this factor ~~and~~ whereas the other 79 % ~~of the data~~ do not specify this

information. These analyses reveal another source of error in the reported *Cp* values, which influences the lack of homogeneity of the results.

3.2. Principal component analysis (PCA) and Response Surface Methodology (RSM)

Finding correlations between the main parameters involved in the *Cp* enhancement is crucial to understand their behavior and giving a step forward to synthesize and optimize NFs. In this study, the three ~~main~~ parameters ~~were~~ selected have been~~:~~ the temperature ~~(°C)~~, the NPs concentration ~~(wt.%),~~ and the NPs size ~~(nm)~~. For this purpose, response surface methodology (RSM) was employed to predict the *Cp* variation (ΔCp, %) and Principal Component Analysis (PCA) was applied to identify the main variables and quantify ~~its~~ their influence on the *Cp* value.

The analysis of the ~~nanofluids~~ dataset by PCA has shown the values of variances~~' values of~~ for the three new PCs, representing the full dataset after the transformation (see **Table 3)**. One criterion for selecting the number of PCs needed is based on the cumulative percentage of the total variance, which is often considered satisfactory when it lies within the range of 70 - 80 % [56]. All the analyzed data in **Table 2** for PC1 and PC2 presents a cumulative percentage of variance > 70 %, which implies that these PCs can be used to explain the dataset, thus reducing the original dimensionality by one variable. Moreover, PCA transformation has shown the correlation between PCs and the original variables (1 means perfect correlation, -1 inverse correlation, and 0 no correlation). While the initial three parameters (concentration, size, and temperature) show approximately the same values for PC1, in PC2, concentration and size are the predominant features. However, the temperature and size have a higher contribution to PC1 and PC2, respectively.

Table 3. Contribution of the original variables to the PCs, Eigenvalues, percentage of variance, and its accumulative values from the PCA analysis.

	PC1	PC2	PC3
Concentration	0.56951	0.627945	0.530418
Size	0.542798	0.771884	0.331007
Temperature	0.617275	0.099399	0.780443
Eigenvalues	1.180865	0.934924	0.892385
Percentage of variance (%)	39.26%	31.08%	29.67%
Cumulative (%)	39.26%	70.33%	100.00%

On the other hand, RSM is a mathematical and statistical technique useful for modeling and problem analysis, where some variables influence the response. The objective is to optimize this response. In this case, the *Cp* is a function of $C_p \cong f(T, \emptyset, S) + \epsilon$, where ϵ represents the noise error observed in the response, T the temperature, $\emptyset$ the concentration, and S the NPs size.

The expected response can be expressed by $E(C_p) = f(T, \emptyset, S) = \beta$ and the response surface can be represented by: $\beta = f(T, \emptyset, S)$ [57]. To obtain the response surface, it is first necessary to find an appropriate approximation of the functional relationship between *Cp* and the independent variables. For this purpose, analysis of variance (ANOVA) was performed. ANOVA provides a statistical test of whether two or more population means are equal and therefore generalizes the *t*-test beyond two means and is based on the analysis of the p-values to predict an optimal response. Therefore, ANOVA analysis should provide a mathematical function for NFs *Cp* values. The p-value represents the smallest level of significance that would lead to the rejection of the null hypothesis, in this case < 0.05 (with a confidence level above 95 %), indicating that the controllable factor does not affect the response [58].

For this propose, several scenarios with different data aggrupation were analyzed:

(1) all the data together,

(2) experimental values,

(3) values obtained under E1269 standard methodology,

(4) values obtained with statistics (sampling and/or repetitions),

(5) values obtained with sampling (> 1 sample),

(6) values obtained with measurement repetitions (> 1 repetition).

In the scenarios (1), (2), (3), (4), and (6), no correlations were found. Therefore, no mathematical model was fitted to the data. Nevertheless, a correlation was found only in the scenario (5) where the obtained *Cp* values ~~is~~ are an average of more than one independent sample (sampling procedure).

Figure 5 shows the ~~three-dimensional~~ 3D predicted response surface ~~(right)~~ and the corresponding contour plot ~~(left)~~ from the ANOVA analysis for the scenario 5. The best model to fit the data ~~was~~ is a quadratic model with p-values lower than ~~<~~0.0001 ~~p-values~~. Moreover, the Model F-value of 6.72 (este valor de qué propiedad es? Especificar!) indicates that the model is significant, and the lack of fit F-value of 0.95 implies that the lack of fit is not significant relative to the pure error. There is only a 0.01 % change that an F-value this large could occur due to noise. Despite this adjustment, the standard deviation of the model is ±7. These deviations agree with Ref. [59]~~previous work~~ where ~~nanofluids'~~ the thermophysical properties of NFs were statistically analyzed by experimental sampling procedures ~~[59]~~. The factors terms were *Cp* (response) = 0.3076 -0.0579· A (temperature) +0.4512 · B (Size) – 1.3651· C (Concentration) –

$0.0004 \cdot AB - 0.0073 \cdot AC + 0.023 \cdot BC + 0.00017 \cdot A^2 - 0.0021 \cdot B^2 - 0.2922 \cdot C^2$. Therefore, this model allows identifying NFs trends. In Figure 5, the predicted *Cp* response as a function of the NPs size and concentration was depicted with the temperature evolution: a-b) at 50ºC, c-d) at 200 ºC, e-f) at 350 ºC and g-h) at 500 ºC. In Figure 5 a-b) at 50 ºC, it can be identified four main regions delimited by the contour lines; from red (+30 % *Cp* variation) to dark blue (- 30% *Cp* variation). Contour lines points to a direction where the *Cp* is maximized. A curved domain with a maximum *Cp* improvement of about 20 % was identified between the NPs concentration range 2 to 9 wt. %, and between 65-100 NPs nominal diameter (nm). In contrast, NP concentration increment leads to a *Cp* variation and NP size decreases, reaching negative values up to -20 %. When the temperature increase (100 - 250 ºC), see Figure 5 c-d) and e-f), the contour lines of 10, 0, and -10 shifted towards high NPs size values; disappearing the domain of values higher than 20 % and appearing new domains of negative values (-20 % and -30 %). On the contrary, with the temperature increase, this trend was changed. At higher temperatures (500 ºC), see Figure 5 g-h) a domain of maximum *Cp* variation is shown up to 25 % for NFs with low NPs concentrations and sizes between 0,001 - 1 wt.% and 30 - 90 nm, respectively. Consequently, a strong temperature dependence has been found in the behavior of NFs. This fact is crucial to select the appropriate parameters (*i.e.,* nanoparticles size and concentration) according to their working temperature. These tendencies are consistent with the values obtained from the PCA analysis.

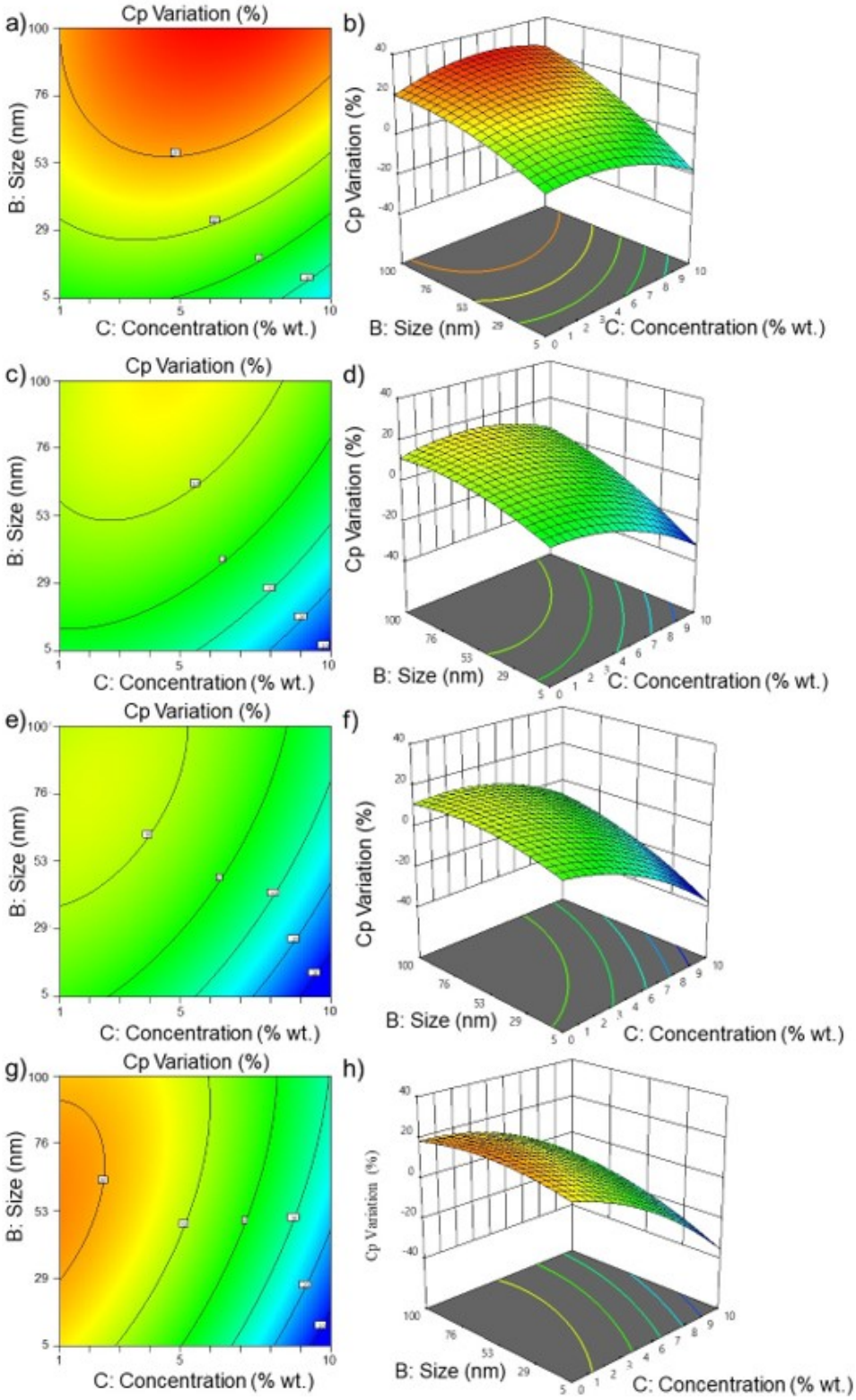

Figure 5. **MEJORAR LA CALIDAD DE LA FIGURA!** ~~A three-dimensional~~ 3D response surface (right) and contour plot (left) showing the expected specific heat capacity (y) as a function of the size (x_1) and concentration (x_2), at a fixed temperature: a)-b) at 50 ºC, c)-d) at 200 ºC, e)-f) at 350 ºC and g)-h) at 500 ºC.

3.3. Nanofluids selector database representation

The relation between the *Cp* variation regarding the initial value, the size, and concentration of NPs, help to understand the connection between the *Cp* change and the NPs addition.

Therefore, creating a database is a helpful way to identify the main trends in NF's behavior. Furthermore, the database makes it possible to define the properties and tolerances of NFs for their in-service engineering modelling/simulation. (i.e., as HTF/TES material in CSP facilities). As seen in the previous sections, the concentration and size of NPs are two of the main significant parameters of NFs thermo-physical properties. Accordingly, a quotient between concentration (wt.%) / size (nm) was defined as an index for NFs: $I^{c/s}$, for better interpretation of the data. In this way, the database makes possible to identify the best parameters for synthetizing NFs with a specific *Cp*. On the other hand, an evidence of the high dispersion of results is elucidated with this database. This fact is observed in the database figures~~:~~ where the higher the bubble size, the higher the dispersion of the data value.

Figure 6 shows the nanofluids Δ*Cp* variations as a function of $I^{c/s}$: **a)** by taking the type of NPs into account and **b)** by base fluids. It can be observed that, generally, metal oxide NPs and carbon base NPs give the most significant variation, particularly, with enhancements up to 150 % when are combined with a molten salt base fluid. These enhancements occur when the $I^{c/s}$ index is between the range of 0.01 - 0.1 wt.% nm^{-1}, (it is important to emphasize that the graphs presented only include spherical shaped nanoparticles when the size is analyzed; nanowires are also included in the database with length x nominal diameter). On the contrary, NFs based on metallic NPs show the worst behavior with variations up to -50 %. Conversely, hydrocarbons, ionic liquids, mixtures, and oils showed a slight positive variation in many cases. However, a severe decrease prevails in many cases with different types of NPs. It is important to highlight that in general, the water base NFs showed a decrease of *Cp*. Therefore, incorporating NPs in water systems does not improve its properties. In the case of substituted hydrocarbons or organic acids are registered enhancements up to 50 %.

Furthermore, in general, the literature's highest Δ*Cp* are obtained with NP~~s~~ concentrations between 0.1 wt.% and ~~up to~~ 2 wt.%. However, some Δ*Cp* enhancements were reported ~~with~~ at higher NPs concentrations~~, an example are~~ as the values ~~reported~~ obtained by Y. Huang *et al.* [60].

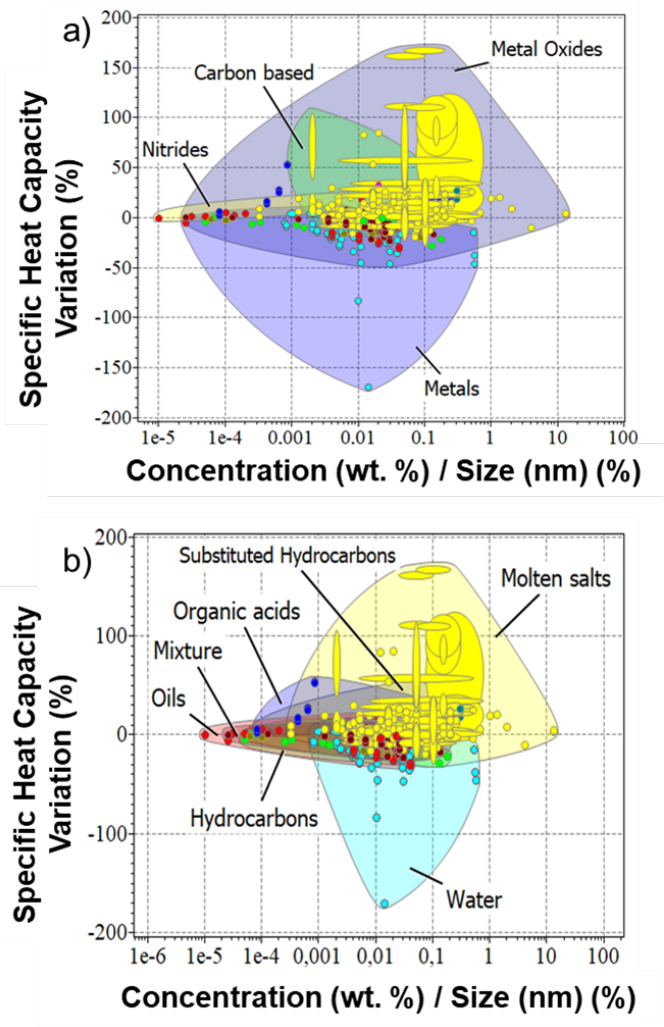

Figure 6. Specific heat capacity variation (%) as a function of the concentration/size ~~quotient~~ ratio ($I^{c/s}$ index) ~~is~~ classified by ~~as~~ a) the nanoparticle~~'s~~ family ~~(a)~~ and ~~classified as~~ b) by the base fluid family. ~~(b).~~

UNIFICAR NUMEROS CON PUNTOS DECIMALES (NO COMAS!!) EN EL EJE X DE LA FIGURA B TIENES COMAS! COMPROBAR TAMBIÉN EN TODO EL TEXTO Y LAS FIGURAS

On the other hand, the size of NPs gives a higher ΔCp enhancement with smaller nominal diameters. For example, from 2 nm to 20 nm of NPs nominal diameter, a significant increase has been observed; whereas, with larger NPs sizes, the increments are less relevant or even negative.

To choose the most suitable NF for a specific application, service temperature is needed to identify the best candidate. **Figure 7** presents the *Cp* values as a function of temperature. In Figure 7-a) are shown the *Cp* of the evaluated NFs versus the measurement temperature. As it can be noted, most NFs reported data is in the temperature range between 25 ºC and 250 ºC. However, molten salts can reach up to 600 ºC. Water, oils, and some mixtures exhibit ~~present~~ the highest *Cp* of the treated NFs, but molten salts are the most employed fluid despite their relatively low *Cp* ~~when working~~ at high temperatures.

For this reason, knowing the *Cp* of this kind of fluids is of great interest. Also, it is essential to consider the *Cp* and the variation that can be achieved by adding NPs. Thus, Figures **7-b)** and **7-c)** represent the Δ*Cp* as a function of temperature, classified as base fluid type, see **7-b)**, and NPs type, see **7-c**).

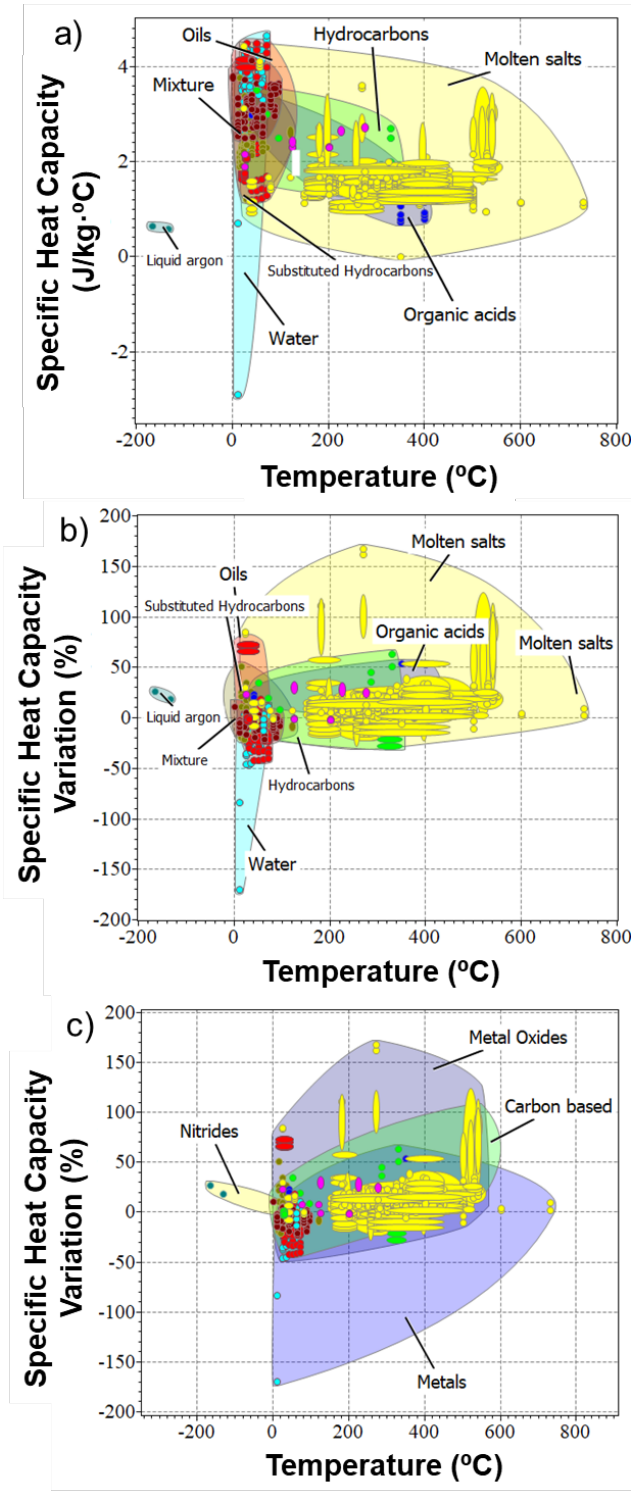

Figure 7. a) Nanofluids specific heat capacity as a function of ~~the~~ temperature~~: for a) specific heat capacity (J/kg·°C) of nanofluids families classified as~~ classified by the type of base fluid ~~type,~~ and ~~b)~~

specific heat capacity variation (%) as a function of temperature classified ~~as the~~ according to the a) base fluid types of family and to the c) ~~Specific heat capacity variation (%) classified as a~~ nanoparticle's family type.

The largest ΔCp are obtained with molten salts at approximately 300 ºC. On the other hand, the second group with higher ΔCp enhancements were thermal oils, reaching improvements up to 80 % with presence of metal oxide NPs. Despite this, they do not exceed the maximum *Cp* values of the water in the temperature range between ambient temperature and 90 ºC.

Finally, **Figure 8** shows a particular case of molten salts and the type of NPs used, ~~from~~ for sizes in the range 1 nm to 200 nm ~~of the nanoparticle size range~~. It can be observed that carbon-based and metal oxides nanoparticles give ~~a~~ the largest~~r~~ *Cp* enhancement, especially at concentrations of NPs between ~~the range of~~ 0.1 to 2 wt.% ~~of NPs~~. Higher variation can be noticed in a particular case of $NaNO_3$-KNO_3 molten salt with MgO as NPs and a concentration of 5, 10, and 15 wt.%, reaching a maximum of *Cp* variation of 168 % [60]–[62]. Otherwise, Li_2CO_3-K_2CO_3 molten salt with SiO_2 NPs also shows a remarkable *Cp* enhancement for concentrations in ~~a~~ the range ~~concentration from~~ 0.1 wt.% to 2 wt.%, achieving ~~a~~ variations in *Cp* between 2 % and 124 % in the experimental results [30], [63]–[69].

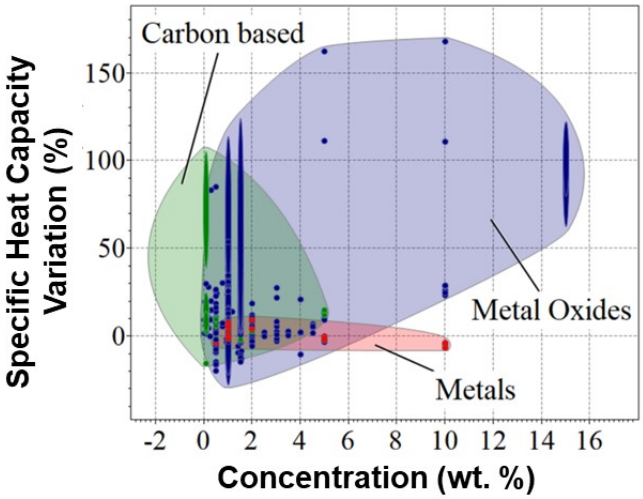

Figure 8. Specific heat capacity variation ~~(%)~~ as a function of concentration of NPs ~~(wt.%) of~~ for molten salt~~s~~-based nanofluids ~~is~~ classified by NP ~~as the nanoparticle's~~ family.

4. Conclusions

This paper collected and analyzed 899 values of nanofluids *Cp* published in the field of thermal energy storage in order to understand their behavior and the effect of incorporating NPs in it. Thanks to the instrumentation analysis, measurement techniques, calculation methods, and the sampling used to determine the *Cp*, the identification of possible sources of errors that cause the large discrepancy in the results presented in the literature have been done. The first identified

source of error was the few methodology specifications in the *Cp* determination. As a result, in a significant part of the reported results there is a gap for a proper methodological procedure for measuring nanofluids thermal properties. The second main source of error was the lack of adequate sampling and statistical analysis. The main conclusions obtained by PCA, RSM methodology, and the database were summarized as the following:

- Temperature, concentration, and NPs size show a similar influence in the *Cp* value.
- A mathematical correlation was determined only with a group of values statistically obtained through a sampling procedure.
- It has been verified that metal oxides NPs are the best candidates for *Cp* enhancements and metal NPs the worst ones. Being the MgO NPs, those who provided increments above 100 %.
- Molten salts were the base fluid with larger *Cp* increments and water with the lowest increment values.
- Higher enhancements were obtained with concentrations from 0.1 wt.% to 2 wt.% and nominal diameter from 2 nm to 20 nm.
  The database allows identifying and selecting nanofluids for specific applications.

5. Recommendations

To sum up, some recommendations for future work are proposed:

(1) To do a statistical sampling procedure and provide a detailed description of this methodology procedure to present a *Cp* value.

(2) To provide not only the *Cp* enhancement but also the nanofluid *Cp* value and the base fluid *Cp* value separately.

(3) To provide information about the *Cp* measurement temperature since it has important influence in the thermophysical properties determination.

All these recommendations facilitate the comparison, and even more important, the reproducibility of the *Cp* values obtained as results and identify NFs behavior patterns and their relationship with the type and concentration of NPs.

Conflict of interest

The authors declare no conflicts of interest.

Acknowledgments

The research leading to these results is partially funded by the Spanish government RTI2018-093849-B-C32, RTI2018-094757-BI00, MDM-2017-0767 MCIU/AEI/FEDER, UE. The authors would like to thank the Catalan Government for the quality accreditation given to their research

groups DIOPMA (2017 SGR 118) and CMSL (2017 SGR 13). DIOPMA is certified agent TECNIO in the category of technology developers from the Government of Catalonia. AS thanks to Generalitat de Catalunya (AGAUR) for her Grant FI-DGR 2018. Moreover, PG thanks Generalitat de Catalunya for his Serra Húnter Associate Professorship. Finally, XS also gratefully acknowledge the financial support of the Science Foundation Ireland 18/EPSRC-CDT/3584 and the Engineering and Physical Sciences Research Council EP/S022635/1, along with VBC Group, Loughborough, UK.

References (FORMATO COMPROBAR FORMATO REVISTA Y UNIFICAR!!!)

[1] Peiró, G., Prieto, C., Gasia, J., Jové, A., Miró, L., and Cabeza, L. F. **2018**. Two-tank molten salts thermal energy storage system for solar power plants at pilot plant scale: Lessons learnt and recommendations for its design, start-up and operation.*Renewable Energy*.vol. 121.pp. 236–248. doi: 10.1016/j.renene.2018.01.026.

[2] Mostafavi Tehrani,S. S.,Taylor,R. A.,Nithyanandam,K.,and Shafiei Ghazani,A. **2017**.Annual comparative performance and cost analysis of high temperature, sensible thermal energy storage systems integrated with a concentrated solar power plant.*Solar Energy*.vol. 153.pp. 153–172. doi: 10.1016/j.solener.2017.05.044.

[3] Calderón,A.,Barreneche,C.,Prieto,C.,Segarra,M.,and Fernández,A. I. **2021**.Concentrating Solar Power Technologies: A Bibliometric Study of Past, Present and Future Trends in Concentrating Solar Power Research.*Frontiers in Mechanical Engineering*.vol. 7, no. June.pp. 1–22. doi: 10.3389/fmech.2021.682592.

[4] Svobodova-Sedlackova,A.,Barreneche,C.,Alonso,G.,Fernandez,A. I.,and Gamallo,P. **2020**.Effect of nanoparticles in molten salts – MD simulations and experimental study.*Renewable Energy*.vol. 152.pp. 208–216. doi: 10.1016/j.renene.2020.01.046.

[5] Peiró,G.,Gasia,J.,Miró,L.,Prieto,C.,and Cabeza,L. F. **2017**.Influence of the heat transfer fluid in a CSP plant molten salts charging process.*Renewable Energy*.vol. 113.pp. 148–158. doi: 10.1016/j.renene.2017.05.083.

[6] Rubbi,F.,Das,L.,Habib,K.,Aslfattahi,N.,Saidur,R.,and Ul Alam,S. **2021**.A comprehensive review on advances of oil-based nanofluids for concentrating solar thermal collector application.*Journal of Molecular Liquids*.no. xxxx.p. 116771. doi: 10.1016/j.molliq.2021.116771.

[7] Minea,A. A. **2021**.State of the art in PEG-based heat transfer fluids and their suspensions with nanoparticles.*Nanomaterials*.vol. 11, no. 1.pp. 1–12. doi: 10.3390/nano11010086.

[8] Wang,W.,Wu,Z.,Li,B.,and Sundén,B. **2019**.A review on molten-salt-based and ionic-liquid-based nanofluids for medium-to-high temperature heat transfer.*Journal of Thermal Analysis and Calorimetry*.vol. 136, no. 3.pp. 1037–1051. doi: 10.1007/s10973-018-7765-y.

[9] Rubbi,F.,Das,L.,Habib,K.,Aslfattahi,N.,Saidur,R.,and Rahman,M. T. **2021**.State-of-the-art review on water-based nanofluids for low temperature solar thermal collector application.*Solar Energy Materials and Solar Cells*.vol. 230, no. June.p. 111220. doi: 10.1016/j.solmat.2021.111220.

[10] Choi,S. U. S.,Li,S.,and Eastman,J. A. **1999**.Measuring thermal conductivity of fluids

containing oxide nanoparticles.*Journal of Heat Transfer*.vol. 121, no. 2.pp. 280–289. doi: 10.1115/1.2825978.

[11] Shi,L.,Zhang,S.,Arshad,A.,Hu,Y.,He,Y.,and Yan,Y. **2021**.Thermo-physical properties prediction of carbon-based magnetic nanofluids based on an artificial neural network.*Renewable and Sustainable Energy Reviews*.vol. 149, no. July 2020.p. 111341. doi: 10.1016/j.rser.2021.111341.

[12] Mukhtar,A. *et al.* **2020**.Experimental and comparative theoretical study of thermal conductivity of MWCNTs-kapok seed oil-based nanofluid.*International Communications in Heat and Mass Transfer*.vol. 110, no. November 2019.p. 104402. doi: 10.1016/j.icheatmasstransfer.2019.104402.

[13] Xiong,Q.,Hajjar,A.,Alshuraiaan,B.,Izadi,M.,Altnji,S.,and Shehzad,S. A. **2021**.State-of-the-art review of nanofluids in solar collectors: A review based on the type of the dispersed nanoparticles.*Journal of Cleaner Production*.vol. 310, no. March.p. 127528. doi: 10.1016/j.jclepro.2021.127528.

[14] Akkala,S. R.,Kaviti,A. K.,ArunKumar,T.,and Sikarwar,V. S. **2021**.Progress on suspended nanostructured engineering materials powered solar distillation- a review.*Renewable and Sustainable Energy Reviews*.vol. 143, no. March.p. 110848. doi: 10.1016/j.rser.2021.110848.

[15] Awais,M.,Bhuiyan,A. A.,Salehin,S.,Ehsan,M. M.,Khan,B.,and Rahman,M. H. **2021**.Synthesis, heat transport mechanisms and thermophysical properties of nanofluids: A critical overview.*International Journal of Thermofluids*.vol. 10.p. 100086. doi: 10.1016/j.ijft.2021.100086.

[16] Sezer,N.,Atieh,M. A.,and Koc,M. **2018**.A comprehensive review on synthesis, stability, thermophysical properties, and characterization of nanofluids.*Powder Technology*.vol. 344.pp. 404–431. doi: 10.1016/j.powtec.2018.12.016.

[17] Sharma,A. K.,Tiwari,A. K.,and Dixit,A. R. **2016**.Rheological behaviour of nanofluids: A review.*Renewable and Sustainable Energy Reviews*.vol. 53.pp. 779–791. doi: 10.1016/j.rser.2015.09.033.

[18] Kumaran,K. **2021**.A comprehensive review on the application of nanofluids in the machining process.*The International Journal of Advanced Manufacturing Technology*.vol. 47. doi: https://doi.org/10.1007/s00170-021-07316-8.

[19] Parmar,H. B. *et al.* **2021**.Nanofluids improve energy efficiency of membrane distillation.*Nano Energy*.vol. 88, no. May.p. 106235. doi: 10.1016/j.nanoen.2021.106235.

[20] Yu,W.,Wang,T.,Park,A. H. A.,and Fang,M. **2019**.Review of liquid nano-absorbents for enhanced CO2 capture.*Nanoscale*.vol. 11, no. 37.pp. 17137–17156. doi: 10.1039/c9nr05089b.

[21] Kim,J. and Park,H. **2021**.Enhanced mass transfer in nanofluid electrolytes for aqueous flow batteries: The mechanism of nanoparticles as catalysts for redox reactions.*Journal of Energy Storage*.vol. 38, no. March.p. 102529. doi: 10.1016/j.est.2021.102529.

[22] Yıldız,G.,Ağbulut,Ü.,and Gürel,A. E. **2021**.A review of stability, thermophysical properties and impact of using nanofluids on the performance of refrigeration systems.*International Journal of Refrigeration*.vol. 129.pp. 342–364. doi: 10.1016/j.ijrefrig.2021.05.016.

[23] Bretado-de los Rios,M. S.,Rivera-Solorio,C. I.,and Nigam,K. D. P. **2021**.An overview of sustainability of heat exchangers and solar thermal applications with nanofluids: A review.*Renewable and Sustainable Energy Reviews*.vol. 142, no. March.p. 110855. doi: 10.1016/j.rser.2021.110855.

[24] Nithiyanantham,U. *et al.* **2019**.Nanoparticles as a high-temperature anticorrosion additive to molten nitrate salts for concentrated solar power.*Solar Energy Materials and Solar Cells*.vol. 203, no. August.p. 110171. doi: 10.1016/j.solmat.2019.110171.

[25] Svobodova-Sedlackova,A.,Calderón,A.,Barreneche,C.,Gamallo,P.,and Fernández,A. I. **2021**.Understanding the abnormal thermal behavior of nanofluids through infrared thermography and thermo - physical characterization.*Scientific Reports*.no. 0123456789.pp. 1–10. doi: 10.1038/s41598-021-84292-9.

[26] Angayarkanni,S. A. and Philip,J. **2015**.Review on thermal properties of nanofluids: Recent developments.*Advances in Colloid and Interface Science*.vol. 225.pp. 146–176. doi: 10.1016/j.cis.2015.08.014.

[27] Lasfargues,M.,Geng,Q.,Cao,H.,and Ding,Y. **2015**.Mechanical dispersion of nanoparticles and its effect on the specific heat capacity of impure binary nitrate salt mixtures.*Nanomaterials*.vol. 5, no. 3.pp. 1136–1146. doi: 10.3390/nano5031136.

[28] Li,Y. *et al.* **2019**.Experimental study on the effect of SiO 2 nanoparticle dispersion on the thermophysical properties of binary nitrate molten salt.*Solar Energy*.vol. 183, no. December 2018.pp. 776–781. doi: 10.1016/j.solener.2019.03.036.

[29] Riazi,H.,Mesgari,S.,Ahmed,N. A.,and Taylor,R. A. **2016**.The effect of nanoparticle morphology on the specific heat of nanosalts.*International Journal of Heat and Mass Transfer*.vol. 94.pp. 254–261. doi: 10.1016/j.ijheatmasstransfer.2015.11.064.

[30] Jiang,Z. *et al.* **2019**.Novel key parameter for eutectic nitrates based nanofluids selection for concentrating solar power (CSP) system.*Applied Energy*.vol. 235, no. July 2018.pp. 529–542. doi: 10.1016/j.apenergy.2018.10.114.

[31] Shahrul,I. M.,Mahbubul,I. M.,Khaleduzzaman,S. S.,Saidur,R.,and Sabri,M. F. M. **2014**.A comparative review on the specific heat of nanofluids for energy perspective.*Renewable and Sustainable Energy Reviews*.vol. 38.pp. 88–98. doi: 10.1016/j.rser.2014.05.081.

[32] Chen,X.,Wu,Y. ting,Zhang,L. di,Wang,X.,and Ma,C. fang. **2019**.Experimental study on thermophysical properties of molten salt nanofluids prepared by high-temperature melting.*Solar Energy Materials and Solar Cells*.vol. 191, no. December 2017.pp. 209–217. doi: 10.1016/j.solmat.2018.11.003.

[33] Pedregosa, Fabian and Varoquaux, Gael and Gramfort, Alexandre and Michel, Vincent and Thirion, Bertrand and Grisel, Olivier and Blondel, Mathieu and Prettenhofer, Peter and Weiss, Ron and Dubourg,V. and others. **2011**.Scikit-learn: Machine Learning in Python.*the Journal of machine Learning research*.vol. 12.pp. 2825–2830. doi: 10.1289/EHP4713.

[34] Jollife,I. T. and Cadima,J. **2016**.Principal component analysis: A review and recent developments.*Philosophical Transactions of the Royal Society A: Mathematical, Physical and Engineering Sciences*.vol. 374, no. 2065. doi: 10.1098/rsta.2015.0202.

[35] Bishop,C. M. **2007**.Pattern Recognition and Machine Learning.*Journal of Electronic Imaging*.vol. 16, no. 4.p. 049901. doi: 10.1117/1.2819119.

[36] Hotelling,H. **1933**.Analysis of a complex of statistical variables into principal components.*Journal of Educational Psychology*.vol. 24, no. 6.pp. 417–441. doi: 10.1037/h0071325.

[37] Che Sidik,N. A.,Mahmud Jamil,M.,Aziz Japar,W. M. A.,and Muhammad Adamu,I. **2017**.A review on preparation methods, stability and applications of hybrid nanofluids.*Renewable and Sustainable Energy Reviews*.vol. 80, no. May.pp. 1112–1122. doi: 10.1016/j.rser.2017.05.221.

[38] Ferrer,G.,Barreneche,C.,Solé,A.,Martorell,I.,and Cabeza,L. F. **2017**.New proposed methodology for specific heat capacity determination of materials for thermal energy storage (TES) by DSC.*Journal of Energy Storage*.vol. 11.pp. 1–6. doi: 10.1016/j.est.2017.02.002.

[39] Mettler Toledo. **1998**.Measuring specific heat capacity.*USER COM*.no. June.pp. 1–20.

[40]. **2018**.*ASTM E1269-11(2018), Standard Test Method for Determining Specific Heat Capacity by Differential Scanning Calorimetry*. West Conshohocken,PA,www.astm.org. [Online]. Available: www.astm.org

[41] ASTM International. **2014**.*ASTM E2716,Standard Test Method for Determining Specific Heat Capacity by Sinusoidal Modulated Temperature Differential Scanning Calorimetry*. West Conshohocken, PA,www.astm.org.

[42] Wang,B. X.,Zhou,L. P.,Peng,X. F.,Du,X. Z.,and Yang,Y. P. **2010**.On the specific heat capacity of CuO nanofluid.*Advances in Mechanical Engineering*.vol. 2010. doi: 10.1155/2010/172085.

[43] Yimin,X. and Wilfried,R. **2000**.Conceptions for heat transfer correlation of nanofluids.*International Journal of Heat and Mass Transfer*.vol. 43, no. 4.pp. 3701–3707. doi: 10.1016/j.aej.2017.01.005.

[44] Pastoriza-Gallego,M. J.,Casanova,C.,Páramo,R.,Barbs,B.,Legido,J. L.,and Piñeiro,M. M. **2009**.A study on stability and thermophysical properties (density and viscosity) of Al2 O3 in water nanofluid.*Journal of Applied Physics*.vol. 106, no. 6. doi: 10.1063/1.3187732.

[45] Vajjha,R. S. and Das,D. K. **2009**.Specific heat measurement of three nanofluids and development of new correlations.*Journal of Heat Transfer*.vol. 131, no. 7.pp. 1–7. doi: 10.1115/1.3090813.

[46] Murshed,S. M. S. **2011**.Determination of effective specific heat of nanofluids.*Journal of Experimental Nanoscience*.vol. 6, no. 5.pp. 539–546. doi: 10.1080/17458080.2010.498838.

[47] Khodadadi,J. M. and Hosseinizadeh,S. F. **2007**.Nanoparticle-enhanced phase change materials (NEPCM) with great potential for improved thermal energy storage.*International Communications in Heat and Mass Transfer*.vol. 34, no. 5.pp. 534–543. doi: 10.1016/j.icheatmasstransfer.2007.02.005.

[48] Rajabpour,A.,Akizi,F.,Heyhat,M.,and Gordiz,K. **2013**.Molecular dynamics simulation of the specific heat capacity of water-Cu nanofluids.*International Nano Letters*.vol. 3, no. 1.p. 58. doi: 10.1186/2228-5326-3-58.

[49] Li,Q.,Yu,Y.,Liu,Y.,Liu,C.,and Lin,L. **2017**.Thermal properties of the mixed n-octadecane/Cu nanoparticle nanofluids during phase transition: A molecular dynamics study.*Materials*.vol. 10, no. 1. doi: 10.3390/ma10010038.

[50] Wang,B.-X.,Zhou,L.-P.,and Peng,X.-F. **2006**.Surface and Size Effects on the Specific Heat Capacity of Nanoparticles.*International Journal of Thermophysics*.vol. 27, no. 1.pp. 139–151. doi: 10.1007/s10765-006-0022-9.

[51] De Robertis,E. *et al.* **2012**.Application of the modulated temperature differential scanning calorimetry technique for the determination of the specific heat of copper nanofluids.*Applied Thermal Engineering*.vol. 41.pp. 10–17. doi: 10.1016/j.applthermaleng.2012.01.003.

[52] Leonard C. Thomas. **2015**.Modulated DSC Paper #1 Why Modulated DSC®? ; An Overview and Summary of Advantages and Disadvantages Relative to Traditional DSC.*TA Instruments Technical Paper*.vol. 1.pp. 1689–1699.

[53] Ma,B.,Kumar,N.,Kuchibhotla,A.,and Banerjee,D. **2018**.Experimental Measurement of the Effect of Particle Concentration on the Specific Heat Capacity of Silica Nanofluids.*Proceedings of the 17th InterSociety Conference on Thermal and Thermomechanical Phenomena in Electronic Systems, ITherm 2018*.pp. 246–251. doi: 10.1109/ITHERM.2018.8419554.

[54] Solé,A.,Miró,L.,Barreneche,C.,Martorell,I.,and Cabeza,L. F. **2013**.Review of the T-history method to determine thermophysical properties of phase change materials (PCM).*Renewable and Sustainable Energy Reviews*.vol. 26.pp. 425–436. doi: 10.1016/j.rser.2013.05.066.

[55] Li,Y.,Zhang,Y.,Li,M.,and Zhang,D. **2013**.Testing method of phase change temperature and heat of inorganic high temperature phase change materials.*Experimental Thermal and Fluid Science*.vol. 44.pp. 697–707. doi: 10.1016/j.expthermflusci.2012.09.010.

[56] Jolliffe,I. T. **2002**.Choosing a subset of principal components or variables, chap. 6, Principal component analysis, 2nd edn., Springer-Verlag, Ed. New York, pp. 111– 149.

[57] Montgomery,D. C. **2013**.*Design and Analysis of Experiments*. John Wiley & Sons, Inc. doi: 10.1002/9783527809080.cataz11063.

[58] Heumann,C. and Schomaker Shalabh,M. **2002**.*Introduction to Statistics and Data Analysis*, no. 1. Springer Nature. doi: 10.1007/978-3-319-46162-5.

[59] Svobodova-Sedlackova,A.,Barreneche,C.,Gamallo,P.,and Inés Fernández,A. **2021**.Novel sampling procedure and statistical analysis for the thermal characterization of ionic nanofluids.*Journal of Molecular Liquids*.vol. 347.p. 118316. doi: 10.1016/j.molliq.2021.118316.

[60] Huang,Y.,Cheng,X.,Li,Y.,Yu,G.,Xu,K.,and Li,G. **2018**.Effect of in-situ synthesized nano-MgO on thermal properties of NaNO3-KNO3.*Solar Energy*.vol. 160, no. December 2017.pp. 208–215. doi: 10.1016/j.solener.2017.11.077.

[61] Navarrete,N. *et al.* **2019**.Improved thermal energy storage of nanoencapsulated phase change materials by atomic layer deposition.*Solar Energy Materials and Solar Cells*.no. October. doi: 10.1016/j.solmat.2019.110322.

[62] Wei,X.,Yin,Y.,Qin,B.,Wang,W.,Ding,J.,and Lu,J. **2020**.Preparation and enhanced thermal conductivity of molten salt nanofluids with nearly unaltered viscosity.*Renewable Energy*.vol. 145.pp. 2435–2444. doi: 10.1016/j.renene.2019.04.153.

[63] Tiznobaik,H. and Shin,D. **2013**.Enhanced specific heat capacity of high-temperature molten salt-based nanofluids.*International Journal of Heat and Mass Transfer*.vol. 57, no. 2.pp. 542–548. doi: 10.1016/j.ijheatmasstransfer.2012.10.062.

[64] Shin,D. and Banerjee,D. **2011**.Enhanced specific heat of silica nanofluid.*Journal of Heat Transfer*.vol. 133, no. 2.pp. 1–4. doi: 10.1115/1.4002600.

[65] Shin,D. and Banerjee,D. **2015**.Enhanced thermal properties of SiO2 nanocomposite for solar thermal energy storage applications.*International Journal of Heat and Mass Transfer*.vol. 84.pp. 898–902. doi: 10.1016/j.ijheatmasstransfer.2015.01.100.

[66] Tiznobaik,H. and Shin,D. **2013**.Experimental validation of enhanced heat capacity of ionic liquid-based nanomaterial.*Applied Physics Letters*.vol. 102, no. 17.pp. 1–4. doi: 10.1063/1.4801645.

[67] Tiznobaik,H. and Shin,D. **2012**.Imece2012-87692 Experimental Study of Nanoengineered Molten Salts As Thermal.pp. 1–6.

[68] Shin,D. and Banerjee,D. **2013**.Enhanced specific heat capacity of nanomaterials

synthesized by dispersing silica nanoparticles in eutectic mixtures.*Journal of Heat Transfer*.vol. 135, no. 3.pp. 1–8. doi: 10.1115/1.4005163.

[69] Shin,D. and Banerjee,D. **2010**.Effects of silica nanoparticles on enhancing the specific heat capacity of carbonate salt eutectic (work in progress).*INTERNATIONAL JOURNAL OF STRUCTURAL CHANGES IN SOLIDS – Mechanics and Applications*.vol. 2, no. November.pp. 25–31. [Online]. Available: http://journals.tdl.org/ijscs/index.php/ijscs/article/view/2337

[70] Lee,J. and Mudawar,I. **2007**.Assessment of the effectiveness of nanofluids for single-phase and two-phase heat transfer in micro-channels.*International Journal of Heat and Mass Transfer*.vol. 50, no. 3–4.pp. 452–463. doi: 10.1016/j.ijheatmasstransfer.2006.08.001.

[71] Assael,M. J.,Antoniadis,K. D.,Wakeham,W. A.,and Zhang,X. **2019**.Potential applications of nanofluids for heat transfer.*International Journal of Heat and Mass Transfer*.vol. 138.pp. 597–607. doi: 10.1016/j.ijheatmasstransfer.2019.04.086.

[72] Selvam,C.,Mohan Lal,D.,and Harish,S. **2017**.Thermal conductivity and specific heat capacity of water–ethylene glycol mixture-based nanofluids with graphene nanoplatelets.*Journal of Thermal Analysis and Calorimetry*.vol. 129, no. 2.pp. 947–955. doi: 10.1007/s10973-017-6276-6.

[73] Ho,C. J.,Huang,J. B.,Tsai,P. S.,and Yang,Y. M. **2011**.Water-based suspensions of Al2O3 nanoparticles and MEPCM particles on convection effectiveness in a circular tube.*International Journal of Thermal Sciences*.vol. 50, no. 5.pp. 736–748. doi: 10.1016/j.ijthermalsci.2010.11.015.

[74] Leela Vinodhan,V.,Suganthi,K. S.,and Rajan,K. S. **2016**.Convective heat transfer performance of CuO-water nanofluids in U-shaped minitube: Potential for improved energy recovery.*Energy Conversion and Management*.vol. 118.pp. 415–425. doi: 10.1016/j.enconman.2016.04.017.

[75] Bock Choon Pak,Y. I. C. **2013**.Hydrodynamic and Heat Transfer Study of Dispersed Fluids With Submicron Metallic Oxide.*Experimental Heat Transfer : A Journal of , Thermal Energy Transport , Storage , and Conversion*.no. January 2013.pp. 37–41.

[76] Carrillo-Berdugo,I. *et al.* **2019**.Interface-inspired formulation and molecular-level perspectives on heat conduction and energy storage of nanofluids.*Scientific Reports*.vol. 9, no. 1.pp. 1–13. doi: 10.1038/s41598-019-44054-0.

[77] Pandey,S. D. and Nema,V. K. **2012**.Experimental analysis of heat transfer and friction factor of nanofluid as a coolant in a corrugated plate heat exchanger.*Experimental Thermal and Fluid Science*.vol. 38.pp. 248–256. doi: 10.1016/j.expthermflusci.2011.12.013.

[78] Ajeel,R. K.,Salim,W. S. W.,and Hasnan,K. **2019**.An experimental investigation of thermal-hydraulic performance of silica nanofluid in corrugated channels.*Advanced Powder Technology*.vol. 30, no. 10.pp. 2262–2275. doi: 10.1016/j.apt.2019.07.006.

[79] Choi,J. and Zhang,Y. **2012**.Numerical simulation of laminar forced convection heat transfer of Al 2O 3-water nanofluid in a pipe with return bend.*International Journal of Thermal Sciences*.vol. 55.pp. 90–102. doi: 10.1016/j.ijthermalsci.2011.12.017.

[80] Teng,T. P. and Hung,Y. H. **2014**.Estimation and experimental study of the density and specific heat for alumina nanofluid.*Journal of Experimental Nanoscience*.vol. 9, no. 7.pp. 707–718. doi: 10.1080/17458080.2012.696219.

[81] Zhou,S. Q. and Ni,R. **2008**.Measurement of the specific heat capacity of water-based Al2 O3 nanofluid.*Applied Physics Letters*.vol. 92, no. 9.pp. 2006–2009. doi: 10.1063/1.2890431.

[82] Khanafer,K.,Vafai,K.,and Lightstone,M. **2003**.Buoyancy-driven heat transfer enhancement in a two-dimensional enclosure utilizing nanofluids.*International Journal of Heat and Mass Transfer*.vol. 46, no. 19.pp. 3639–3653. doi: 10.1016/S0017-9310(03)00156-X.

[83] Pantzali,M. N.,Kanaris,A. G.,Antoniadis,K. D.,Mouza,A. A.,and Paras,S. V. **2009**.Effect of nanofluids on the performance of a miniature plate heat exchanger with modulated surface.*International Journal of Heat and Fluid Flow*.vol. 30, no. 4.pp. 691–699. doi: 10.1016/j.ijheatfluidflow.2009.02.005.

[84] Barbés,B. *et al.* **2013**.Thermal conductivity and specific heat capacity measurements of Al 2O3 nanofluids.*Journal of Thermal Analysis and Calorimetry*.vol. 111, no. 2.pp. 1615–1625. doi: 10.1007/s10973-012-2534-9.

[85] O'Hanley,H.,Buongiorno,J.,McKrell,T.,and Hu,L. W. **2012**.Measurement and model validation of nanofluid specific heat capacity with differential scanning calorimetry.*Advances in Mechanical Engineering*.vol. 2012. doi: 10.1155/2012/181079.

[86] Martín,M.,Villalba,A.,Inés Fernández,A.,and Barreneche,C. **2019**.Development of new nano-enhanced phase change materials (NEPCM) to improve energy efficiency in buildings: Lab-scale characterization.*Energy and Buildings*.vol. 192.pp. 75–83. doi: 10.1016/j.enbuild.2019.03.029.

[87] Gunjo,D. G.,Jena,S. R.,Mahanta,P.,and Robi,P. S. **2018**.Melting enhancement of a latent heat storage with dispersed Cu, CuO and Al2O3 nanoparticles for solar thermal application.*Renewable Energy*.vol. 121.pp. 652–665. doi: 10.1016/j.renene.2018.01.013.

[88] Sebti,S. S.,Mastiani,M.,Mirzaei,H.,Dadvand,A.,Kashani,S.,and Hosseini,S. A. **2013**.Numerical study of the melting of nano-enhanced phase change material in a square cavity.*Journal of Zhejiang University: Science A*.vol. 14, no. 5.pp. 307–316. doi: 10.1631/jzus.A1200208.

[89] Wu,S.,Wang,H.,Xiao,S.,and Zhu,D. **2012**.Numerical simulation on thermal energy storage behavior of Cu/paraffin nanofluids PCMs.*Procedia Engineering*.vol. 31.pp. 240–244. doi: 10.1016/j.proeng.2012.01.1018.

[90] Starace,A. K.,Gomez,J. C.,Wang,J.,Pradhan,S.,and Glatzmaier,G. C. **2011**.Nanofluid heat capacities.*Journal of Applied Physics*.vol. 110, no. 12. doi: 10.1063/1.3672685.

[91] Nelson,I. C.,Banerjee,D.,and Ponnappan,R. **2009**.Flow loop experiments using polyalphaolefin nanofluids.*Journal of Thermophysics and Heat Transfer*.vol. 23, no. 4.pp. 752–761. doi: 10.2514/1.31033.

[92] Ghazvini,M.,Akhavan-Behabadi,M. A.,Rasouli,E.,and Raisee,M. **2012**.Heat transfer properties of nanodiamond-engine oil nanofluid in laminar flow.*Heat Transfer Engineering*.vol. 33, no. 6.pp. 525–532. doi: 10.1080/01457632.2012.624858.

[93] Saeedinia,M.,Akhavan-Behabadi,M. A.,and Razi,P. **2012**.Thermal and rheological characteristics of CuO-Base oil nanofluid flow inside a circular tube.*International Communications in Heat and Mass Transfer*.vol. 39, no. 1.pp. 152–159. doi: 10.1016/j.icheatmasstransfer.2011.08.001.

[94] Murshed,S. M. S. **2012**.Simultaneous measurement of thermal conductivity, thermal diffusivity, and specific heat of nanofluids.*Heat Transfer Engineering*.vol. 33, no. 8.pp. 722–731. doi: 10.1080/01457632.2011.635986.

[95] Fakoor Pakdaman,M.,Akhavan-Behabadi,M. A.,and Razi,P. **2012**.An experimental investigation on thermo-physical properties and overall performance of MWCNT/heat transfer oil nanofluid flow inside vertical helically coiled tubes.*Experimental Thermal and Fluid Science*.vol. 40.pp. 103–111. doi: 10.1016/j.expthermflusci.2012.02.005.

[96] Toghyani,S.,Baniasadi,E.,and Afshari,E. **2016**.Thermodynamic analysis and optimization of an integrated Rankine power cycle and nano-fluid based parabolic trough solar collector.*Energy Conversion and Management*.vol. 121.pp. 93–104. doi: 10.1016/j.enconman.2016.05.029.

[97] Dehury,P.,Singh,J.,and Banerjee,T. **2018**.Thermophysical and Forced Convection Studies on (Alumina + Menthol)-Based Deep Eutectic Solvents for Their Use as a Heat Transfer Fluid.*ACS Omega*.vol. 3, no. 12.pp. 18016–18027. doi: 10.1021/acsomega.8b02661.

[98] Wang,B. X.,Zhou,L. P.,Peng,X. F.,Du,X. Z.,and Yang,Y. P. **2010**.On the specific heat capacity of CuO nanofluid.*Advances in Mechanical Engineering*.vol. 2010, no. January. doi: 10.1155/2010/172085.

[99] Akilu,S.,Baheta,A. T.,Minea,A. A.,and Sharma,K. V. **2017**.Rheology and thermal conductivity of non-porous silica (SiO2) in viscous glycerol and ethylene glycol based nanofluids.*International Communications in Heat and Mass Transfer*.vol. 88, no. October.pp. 245–253. doi: 10.1016/j.icheatmasstransfer.2017.08.001.

[100] Teng,T. P. and Yu,C. C. **2013**.Heat dissipation performance of MWCNTs nano-coolant for vehicle.*Experimental Thermal and Fluid Science*.vol. 49.pp. 22–30. doi: 10.1016/j.expthermflusci.2013.03.007.

[101] Nieh,H. M.,Teng,T. P.,and Yu,C. C. **2014**.Enhanced heat dissipation of a radiator using oxide nano-coolant.*International Journal of Thermal Sciences*.vol. 77.pp. 252–261. doi: 10.1016/j.ijthermalsci.2013.11.008.

[102] Kumaresan,V. and Velraj,R. **2012**.Experimental investigation of the thermo-physical properties of water-ethylene glycol mixture based CNT nanofluids.*Thermochimica Acta*.vol. 545.pp. 180–186. doi: 10.1016/j.tca.2012.07.017.

[103] Kumaresan,V.,Mohaideen Abdul Khader,S.,Karthikeyan,S.,and Velraj,R. **2013**.Convective heat transfer characteristics of CNT nanofluids in a tubular heat exchanger of various lengths for energy efficient cooling/heating system.*International Journal of Heat and Mass Transfer*.vol. 60, no. 1.pp. 413–421. doi: 10.1016/j.ijheatmasstransfer.2013.01.021.

[104] Nagarajan,F. C.,Kannaiyan,S. K.,and Boobalan,C. **2020**.Intensification of heat transfer rate using alumina-silica nanocoolant.*International Journal of Heat and Mass Transfer*.vol. 149. doi: 10.1016/j.ijheatmasstransfer.2019.119127.

[105] Kulkarni,D. P.,Vajjha,R. S.,Das,D. K.,and Oliva,D. **2008**.Application of aluminum oxide nanofluids in diesel electric generator as jacket water coolant.*Applied Thermal Engineering*.vol. 28, no. 14–15.pp. 1774–1781. doi: 10.1016/j.applthermaleng.2007.11.017.

[106] Vajjha,R. S. and Das,D. K. **2012**.A review and analysis on influence of temperature and concentration of nanofluids on thermophysical properties, heat transfer and pumping power.*International Journal of Heat and Mass Transfer*.vol. 55, no. 15–16.pp. 4063–4078. doi: 10.1016/j.ijheatmasstransfer.2012.03.048.

[107] P.K.,Na.,D.P.,K.,A.,D.,and D.K.,D. **2007**.Experimental investigation of viscosity and specific heat of silicon dioxide nanofluid.*Micro and Nano Letters*.vol. 2, no. 3.pp. 67–71. doi: 10.1049/mnl.

[108] Elias,M. M. *et al.* **2014**.Experimental investigation on the thermo-physical properties of Al2O3 nanoparticles suspended in car radiator coolant.*International Communications in Heat and Mass Transfer*.vol. 54.pp. 48–53. doi: 10.1016/j.icheatmasstransfer.2014.03.005.

[109] Qiao,G.,Lasfargues,M.,Alexiadis,A.,and Ding,Y. **2017**.Simulation and experimental

study of the specific heat capacity of molten salt based nanofluids.*Applied Thermal Engineering*.vol. 111.pp. 1517–1522. doi: 10.1016/j.applthermaleng.2016.07.159.

[110] Awad,A.,Navarro,H.,Ding,Y.,and Wen,D. **2018**.Thermal-physical properties of nanoparticle-seeded nitrate molten salts.*Renewable Energy*.vol. 120.pp. 275–288. doi: 10.1016/j.renene.2017.12.026.

[111] Chieruzzi,M.,Miliozzi,A.,Crescenzi,T.,Torre,L.,and Kenny,J. M. **2015**.A New Phase Change Material Based on Potassium Nitrate with Silica and Alumina Nanoparticles for Thermal Energy Storage.*Nanoscale Research Letters*.vol. 10, no. 1. doi: 10.1186/s11671-015-0984-2.

[112] Dudda,B. and Shin,D. **2012**.Imece2012-87707 Investigation of Molten Salt Nanomaterial As Thermal Energy Storage in.pp. 1–6.

[113] Muñoz-Sánchez,B.,Nieto-Maestre,J.,Iparraguirre-Torres,I.,Julià,J. E.,and García-Romero,A. **2017**.Silica and alumina nano-enhanced molten salts for thermal energy storage: A comparison.*AIP Conference Proceedings*.vol. 1850, no. June. doi: 10.1063/1.4984439.

[114] Nithiyanantham,U.,Grosu,Y.,González-Fernández,L.,Zaki,A.,Igartua,J. M.,and Faik,A. **2019**.Development of molten nitrate salt based nanofluids for thermal energy storage application: High thermal performance and long storage components life-time.*SOLARPACES 2018: International Conference on Concentrating Solar Power and Chemical Energy Systems*.vol. 2126.p. 200025. doi: 10.1063/1.5117740.

[115] Hu,Y.,Zhang,B.,Tan,K.,He,Y.,and Zhu,J. **2020**.Regulation of natural convection heat transfer for SiO2–solar salt nanofluids by optimizing rectangular vessels design.*Asia-Pacific Journal of Chemical Engineering*.no. January.pp. 1–15. doi: 10.1002/apj.2409.

[116] Dudda,B. and Shin,D. **2013**.Effect of nanoparticle dispersion on specific heat capacity of a binary nitrate salt eutectic for concentrated solar power applications.*International Journal of Thermal Sciences*.vol. 69.pp. 37–42. doi: 10.1016/j.ijthermalsci.2013.02.003.

[117] Andreu-Cabedo,P.,Mondragon,R.,Hernandez,L.,Martinez-Cuenca,R.,Cabedo,L.,and Julia,J. E. **2014**.Increment of specific heat capacity of solar salt with SiO2 nanoparticles.*Nanoscale Research Letters*.vol. 9, no. 1.pp. 1–11. doi: 10.1186/1556-276X-9-582.

[118] Navarrete,N.,Hernández,L.,Vela,A.,and Mondragón,R. **2020**.Influence of the production method on the thermophysical properties of high temperature molten salt-based nanofluids.*Journal of Molecular Liquids*.vol. 302.p. 112570. doi: 10.1016/j.molliq.2020.112570.

[119] Hu,Y.,He,Y.,Gao,H.,and Zhang,Z. **2019**.Forced convective heat transfer characteristics of solar salt-based SiO2 nanofluids in solar energy applications.*Applied Thermal Engineering*.vol. 155, no. April.pp. 650–659. doi: 10.1016/j.applthermaleng.2019.04.109.

[120] Chieruzzi,M.,Cerritelli,G. F.,Miliozzi,A.,Kenny,J. M.,and Torre,L. **2017**.Heat capacity of nanofluids for solar energy storage produced by dispersing oxide nanoparticles in nitrate salt mixture directly at high temperature.*Solar Energy Materials and Solar Cells*.vol. 167, no. December 2016.pp. 60–69. doi: 10.1016/j.solmat.2017.04.011.

[121] Hu,Y.,He,Y.,Zhang,Z.,and Wen,D. **2019**.Enhanced heat capacity of binary nitrate eutectic salt-silica nanofluid for solar energy storage.*Solar Energy Materials and Solar Cells*.vol. 192, no. July 2018.pp. 94–102. doi: 10.1016/j.solmat.2018.12.019.

[122] Muñoz-Sánchez,B.,Nieto-Maestre,J.,Iparraguirre-Torres,I.,Sánchez-García,J. A.,Julia,J. E.,and García-Romero,A. **2016**.The influence of mixing water on the thermophysical properties of nanofluids based on solar salt and silica nanoparticles.*AIP Conference*

Proceedings.vol. 1734, no. May 2016. doi: 10.1063/1.4949129.

[123] Muñoz-Sánchez,B.,Nieto-Maestre,J.,Guerreiro,L.,Julia,J. E.,Collares-Pereira,M.,and García-Romero,A. **2017**.Molten salt based nanofluids based on solar salt and alumina nanoparticles: An industrial approach.*AIP Conference Proceedings*.vol. 1850, no. June. doi: 10.1063/1.4984437.

[124] Schuller,M.,Shao,Q.,and Lalk,T. **2015**.Experimental investigation of the specific heat of a nitrate-alumina nanofluid for solar thermal energy storage systems.*International Journal of Thermal Sciences*.vol. 91.pp. 142–145. doi: 10.1016/j.ijthermalsci.2015.01.012.

[125] Lu,M.-C. and Huang,C.-H. **2013**.Specific heat capacity of molten salt-based alumina nanofluid.*Nanoscale research letters*.vol. 8, no. 1.p. 292. doi: 10.1186/1556-276X-8-292.

[126] Nithiyanantham,U.,González-Fernández,L.,Grosu,Y.,Zaki,A.,Igartua,J. M.,and Faik,A. **2020**.Shape effect of Al2O3 nanoparticles on the thermophysical properties and viscosity of molten salt nanofluids for TES application at CSP plants.*Applied Thermal Engineering*.vol. 169, no. January.p. 114942. doi: 10.1016/j.applthermaleng.2020.114942.

[127] Chieruzzi,M.,Cerritelli,G. F.,Miliozzi,A.,and Kenny,J. M. **2013**.Effect of nanoparticles on heat capacity of nanofluids based on molten salts as PCM for thermal energy storage.*Nanoscale Research Letters*.vol. 8, no. 1.pp. 1–9. doi: 10.1186/1556-276X-8-448.

[128] Muñoz-Sánchez,B.,Nieto-Maestre,J.,Imbuluzqueta,G.,Marañón,I.,Iparraguirre-Torres,I.,and García-Romero,A. **2017**.A precise method to measure the specific heat of solar salt-based nanofluids.*Journal of Thermal Analysis and Calorimetry*.vol. 129, no. 2.pp. 905–914. doi: 10.1007/s10973-017-6272-x.

[129] Hu,Y.,He,Y.,Zhang,Z.,and Wen,D. **2017**.Effect of Al2O3 nanoparticle dispersion on the specific heat capacity of a eutectic binary nitrate salt for solar power applications.*Energy Conversion and Management*.vol. 142.pp. 366–373. doi: 10.1016/j.enconman.2017.03.062.

[130] Lasfargues,M.,Bell,A.,and Ding,Y. **2016**.In situ production of titanium dioxide nanoparticles in molten salt phase for thermal energy storage and heat-transfer fluid applications.*Journal of Nanoparticle Research*.vol. 18, no. 6.pp. 1–11. doi: 10.1007/s11051-016-3460-8.

[131] Navarrete,N.,Mondragón,R.,Wen,D.,Navarro,M. E.,Ding,Y.,and Juliá,J. E. **2019**.Thermal energy storage of molten salt –based nanofluid containing nano-encapsulated metal alloy phase change materials.*Energy*.vol. 167.pp. 912–920. doi: 10.1016/j.energy.2018.11.037.

[132] Lasfargues,M.,Stead,G.,Amjad,M.,Ding,Y.,and Wen,D. **2017**.In situ production of copper oxide nanoparticles in a binary molten salt for concentrated solar power plant applications.*Materials*.vol. 10, no. 5.pp. 1–10. doi: 10.3390/ma10050537.

[133] Luo,Y.,Du,X.,Awad,A.,and Wen,D. **2017**.Thermal energy storage enhancement of a binary molten salt via in-situ produced nanoparticles.*International Journal of Heat and Mass Transfer*.vol. 104.pp. 658–664. doi: 10.1016/j.ijheatmasstransfer.2016.09.004.

[134] Xie,Q.,Zhu,Q.,and Li,Y. **2016**.Thermal Storage Properties of Molten Nitrate Salt-Based Nanofluids with Graphene Nanoplatelets.*Nanoscale Research Letters*.vol. 11, no. 1.pp. 1–7. doi: 10.1186/s11671-016-1519-1.

[135] Hamdy,E.,Ebrahim,S.,Abulfotuh,F.,and Soliman,M. **2017**.Effect of multi-walled carbon nanotubes on thermal properties of nitrate molten salts.*Proceedings of 2016 International Renewable and Sustainable Energy Conference, IRSEC 2016*.pp. 317–320. doi: 10.1109/IRSEC.2016.7983997.

[136] Hassan,M. A. and Banerjee,D. **2019**.A soft computing approach for estimating the specific heat capacity of molten salt-based nanofluids.*Journal of Molecular Liquids*.vol. 281.pp. 365–375. doi: 10.1016/j.molliq.2019.02.106.

[137] He,Q.,Wang,S.,Tong,M.,and Liu,Y. **2012**.Experimental study on thermophysical properties of nanofluids as phase-change material (PCM) in low temperature cool storage.*Energy Conversion and Management*.vol. 64.pp. 199–205. doi: 10.1016/j.enconman.2012.04.010.

[138] Tian,H. *et al.* **2017**.Enhanced specific heat capacity of binary chloride salt by dissolving magnesium for higherature thermal energy storage and transfer.*Journal of Materials Chemistry A*.vol. 5, no. 28.pp. 14811–14818. doi: 10.1039/c7ta04169a.

[139] Shin,D. and Banerjee,D. **2011**.Enhancement of specific heat capacity of high-temperature silica-nanofluids synthesized in alkali chloride salt eutectics for solar thermal-energy storage applications.*International Journal of Heat and Mass Transfer*.vol. 54, no. 5–6.pp. 1064–1070. doi: 10.1016/j.ijheatmasstransfer.2010.11.017.

[140] Chen,X.,Wu,Y. ting,Zhang,L. di,Wang,X.,and Ma,C. fang. **2018**.Experimental study on the specific heat and stability of molten salt nanofluids prepared by high-temperature melting.*Solar Energy Materials and Solar Cells*.vol. 176, no. November 2017.pp. 42–48. doi: 10.1016/j.solmat.2017.11.021.

[141] Zhang,L. di,Chen,X.,Wu,Y. ting,Lu,Y. wei,and Ma,C. fang. **2016**.Effect of nanoparticle dispersion on enhancing the specific heat capacity of quaternary nitrate for solar thermal energy storage application.*Solar Energy Materials and Solar Cells*.vol. 157.pp. 808–813. doi: 10.1016/j.solmat.2016.07.046.

[142] Liu,Y. and Yang,Y. **2017**.Investigation of specific heat and latent heat enhancement in hydrate salt based TiO2 nanofluid phase change material.*Applied Thermal Engineering*.vol. 124.pp. 533–538. doi: 10.1016/j.applthermaleng.2017.05.150.

[143] Ho,M. X. and Pan,C. **2014**.Optimal concentration of alumina nanoparticles in molten hitec salt to maximize its specific heat capacity.*International Journal of Heat and Mass Transfer*.vol. 70.pp. 174–184. doi: 10.1016/j.ijheatmasstransfer.2013.10.078.

[144] Sang,L.,Ai,W.,Liu,T.,Wu,Y.,and Ma,C. **2019**.Insights into the specific heat capacity enhancement of ternary carbonate nanofluids with SiO 2 nanoparticles: the effect of change in the composition ratio.*RSC Advances*.vol. 9, no. 10.pp. 5288–5294. doi: 10.1039/c8ra10318f.

[145] Shin,D. and Banerjee,D. **2014**.Specific heat of nanofluids synthesized by dispersing alumina nanoparticles in alkali salt eutectic.*International Journal of Heat and Mass Transfer*.vol. 74.pp. 210–214. doi: 10.1016/j.ijheatmasstransfer.2014.02.066.

[146] Jo,B. and Banerjee,D. **2014**.Enhanced specific heat capacity of molten salt-based nanomaterials: Effects of nanoparticle dispersion and solvent material.*Acta Materialia*.vol. 75.pp. 80–91. doi: 10.1016/j.actamat.2014.05.005.

[147] Tiznobaik,H.,Banerjee,D.,and Shin,D. **2015**.Effect of formation of “long range” secondary dendritic nanostructures in molten salt nanofluids on the values of specific heat capacity.*International Journal of Heat and Mass Transfer*.vol. 91.pp. 342–346. doi: 10.1016/j.ijheatmasstransfer.2015.05.072.

[148] Jo,B. and Banerjee,D. **2015**.Enhanced specific heat capacity of molten salt-based carbon nanotubes nanomaterials.*Journal of Heat Transfer*.vol. 137, no. 9.pp. 1–7. doi: 10.1115/1.4030226.

[149] Jo,B. and Banerjee,D. **2014**.Enhanced specific heat capacity of molten salts using organic nanoparticles.no. 2011.pp. 1–8.

[150] Seo,J. and Shin,D. **2014**.Enhancement of specific heat of ternary nitrate (LiNO3-NaNO3-KNO3) salt by doping with SiO2 nanoparticles for solar thermal energy storage.*Micro and Nano Letters*.vol. 9, no. 11.pp. 817–820. doi: 10.1049/mnl.2014.0407.

[151] Seo,J. and Shin,D. **2016**.Size effect of nanoparticle on specific heat in a ternary nitrate (LiNO3-NaNO3-KNO3) salt eutectic for thermal energy storage.*Applied Thermal Engineering*.vol. 102.pp. 144–148. doi: 10.1016/j.applthermaleng.2016.03.134.

[152] Sonawane,S.,Patankar,K.,Fogla,A.,Puranik,B.,Bhandarkar,U.,and Sunil Kumar,S. **2011**.An experimental investigation of thermo-physical properties and heat transfer performance of Al2O3-Aviation Turbine Fuel nanofluids.*Applied Thermal Engineering*.vol. 31, no. 14–15.pp. 2841–2849. doi: 10.1016/j.applthermaleng.2011.05.009.

[153] Nieto De Castro,C. A.,Murshed,S. M. S.,Lourenço,M. J. V.,Santos,F. J. V.,Lopes,M. L. M.,and França,J. M. P. **2012**.Enhanced thermal conductivity and specific heat capacity of carbon nanotubes ionanofluids.*International Journal of Thermal Sciences*.vol. 62.pp. 34–39. doi: 10.1016/j.ijthermalsci.2012.03.010.

[154] Liu,J.,Wang,F.,Zhang,L.,Fang,X.,and Zhang,Z. **2014**.Thermodynamic properties and thermal stability of ionic liquid-based nanofluids containing graphene as advanced heat transfer fluids for medium-to-high-temperature applications.*Renewable Energy*.vol. 63.pp. 519–523. doi: 10.1016/j.renene.2013.10.002.

[155] Paul,T. C.,Morshed,A. K. M. M.,and Khan,J. A. **2013**.Nanoparticle Enhanced Ionic Liquids (NEILS) as working fluid for the next generation solar collector.*Procedia Engineering*.vol. 56.pp. 631–636. doi: 10.1016/j.proeng.2013.03.170.

[156] Mohebbi,A. **2012**.Prediction of specific heat and thermal conductivity of nanofluids by a combined equilibrium and non-equilibrium molecular dynamics simulation.*Journal of Molecular Liquids*.vol. 175.pp. 51–58. doi: 10.1016/j.molliq.2012.08.010.